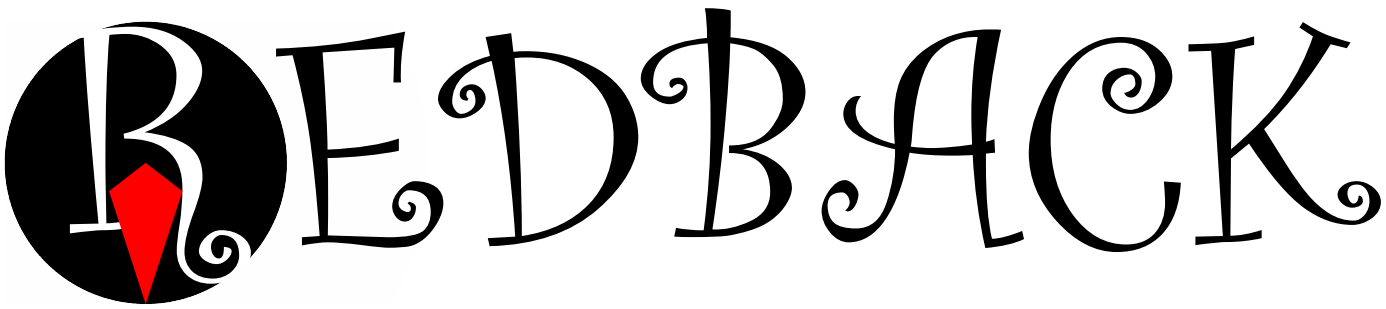

Open–source software for efficient noise–reduction in plate kinematic reconstructions.

User manual

Version released on November 12, 2015

Contents

1 Introduction **3**

2 Download and installation **4**

3 Algorithm **4**

4 Inputs to REDBACK **5**
4.1 Finite rotations file . . . 5
4.2 Parameters file . . . 7

5 Setting the parameters and running REDBACK **7**
5.1 Parameters setting . . . 7
5.2 Running REDBACK . . . 10

6 Outputs from REDBACK **12**

7 Post–simulation diagnostics **13**

8 An example of running REDBACK **15**
8.1 Step 1 . . . 15
8.2 Step 2 . . . 17
8.3 Step 3 . . . 18
8.4 Step 4 . . . 19
8.5 Step 5 . . . 20
8.6 Step 6 . . . 21
8.7 Step 7 . . . 22
8.8 Step 8 . . . 23
8.9 Step 9 . . . 24
8.10 Step 10 . . . 25
8.11 Step 11 . . . 26
8.12 Step 12 . . . 27
8.13 Step 13 . . . 28
8.14 Step 14 . . . 29
8.15 Step 15 . . . 30
8.16 Step 16 . . . 31
8.17 Step 17 . . . 32
8.18 Step 18 . . . 33
8.19 Step 19 . . . 34
8.20 Step 20 . . . 35
8.21 Step 21 . . . 36
8.22 Step 22 . . . 37

9 Final remarks **41**

10 Appendix A: Updates history **42**

1 Introduction

REDBACK is software for efficient reduction of noise in finite–rotation data sets, which allow reconstructing Earth's past plate motions. It has been developed at the Research School of Earth Sciences (RSES) of the Australian National University (ANU) as part of the AuScope–AGOS Inversion Laboratory, and is released as open–source under the GNU General Public License (GPL – http://www.gnu.org/licenses/gpl.html).

REDBACK has been designed to run on personal computers. It is available for Unix (Linux and Mac OS), but can also run under Windows via a terminal emulator (e.g. Cygwin – http://cygwin.com). Its strengths are easiness of use and computational efficiency. Users include plate kinematicists, geodynamicists and, more generally, anyone making use of tectonic plate motions and their changes through geological time.

REDBACK implements trans–dimensional hierarchical Bayesian Inference [see *Iaffaldano et al.*, 2012, 2014, and references therein for more details]. This user manual explains how to obtain, install and run REDBACK. The manual builds on the development by *Iaffaldano et al.* [2012, 2014], which you are encouraged to read beforehand.

We emphasise that in Bayesian Inference, users need to make choices in order to obtain a reliable solution to the problem at hand. For this reason, REDBACK features a small number of parameters that you will need to set and adjust. A significant portion of this manual is dedicated to explaining what these parameters are and what their impact is on the final solution. Importantly, we do so by resorting to an example based on real finite rotations. It illustrates how the parameter selection should be carried out, in order to obtain a robust solution.

REDBACK was built with programming support from the *Inversion Laboratory*, which is part of the Australian Geophysical Observing System (AGOS) funded by Auscope Ltd.

We hope the Earth Science community will find REDBACK a useful tool to interpret observations and advance our understanding of a range of geological processes.

Giampiero Iaffaldano
Rhys Hawkins
Thomas Bodin
Malcolm Sambridge
Canberra, February 2014.

2 Download and installation

REDBACK can be obtained by logging onto http://www.iearth.org.au/codes/REDBACK, or by contacting Giampiero Iaffaldano at RSES–ANU (giampiero.iaffaldano@anu.edu.au). A copy of the GNU GPL is also available at the link above, as well as within the installation package. In order to download REDBACK, we ask that you register as a user, so that you may be notified of updates in the future.

The installation package, of which this manual is part, consists of two compressed folders: RJMCMC-#.tar.gz (the symbol # indicates the version currently available for download) and REDBACK-#.tar.gz. The latter is the actual software for reduction of finite–rotation noise, while the former is a software library for the Reversible Jump Monte–Carlo Markov Chain, which REDBACK uses. In order to compile REDBACK, you need to have the GCC compiler collection already installed on your machine. This is available for download at http://gcc.gnu.org/.

You can install and run REDBACK and RJMCMC from any Unix shell (e.g. Terminal on Linux; Terminal.app or X11.app on Mac OS X; emulators such as Cygwin on WINDOWS). In particular, if you intend to use Cygwin under Windows, we recommend that you request the following packages to be included during the installation of Cygwin: `gcc-fortran`, `autoconf`, `automake` and `pkgconfig`.

After downloading and decompressing the RJMCMC-#.tar.gz and REDBACK-#.tar.gz, open a terminal window and move to `RJMCMC/` to install the associated library. The file `README` within it explains how to do so. This essentially involves entering the following three commands:

```
./configure
make
sudo make install
```

At the end of the installation of the RJMCMC library, the path to the installation folder is prompted to the terminal (highlighted in light blue in Figure 1). Take note of such a path, as it may be needed to install REDBACK.

Once the RJMCMC library has been installed, move to `REDBACK/` and open `README` in it, to get instructions for installation of REDBACK. Note that if RJMCMC has been installed within one of the common locations, REDBACK will automatically detect it during installation. However, if this is not the case the installation will fail. For this reason, we recommend that you provide the path to the RJMCMC library to REDBACK. This is easily achieved by typing the following sequence of commands for installations:

`export PKG_CONFIG_PATH=`'RJMCMC PATH' (in Figure 1 'RJMCMC PATH' is `/usr/local/lib/pkgconfig`)
`./configure`
`make`
`sudo make install`

3 Algorithm

See *Iaffaldano et al.* [2012, 2014, and references therein] for a comprehensive description of the algorithm for trans–dimensional hierarchical Bayesian Inference that is implemented in REDBACK. Here we shall only mention that REDBACK provides independent solutions for the temporal series of rotated angle on the one hand, and rotation pole on the other. These are then combined to obtain a temporal series of stage Euler vectors (or simply Euler vectors) [e.g. *Cox and Hart*, 1986].

The rationale for doing so stems from the fact that a plate–motion change may correspond to (i) a change in the angular velocity, (ii) a change in the position of the stage rotation axis, or (iii) both simultaneously. These types of plate kinematic change will be mapped into finite rotations as, respectively, a change in the rate at which the rotated angle varies through time, a pronounced shift of the finite–rotation pole, or both simultaneously. In our opinion it makes therefore sense to independently reduce noise from the temporal series of rotated angle and rotation pole.

```
Making install in src
 .././install-sh -c -d '/usr/local/lib'
 /bin/sh ../libtool   --mode=install /usr/bin/install -c   librjmcmc.la '/usr/local/lib'
libtool: install: /usr/bin/install -c .libs/librjmcmc.0.dylib /usr/local/lib/librjmcmc.0.d
ylib
libtool: install: (cd /usr/local/lib && { ln -s -f librjmcmc.0.dylib librjmcmc.dylib || {
rm -f librjmcmc.dylib && ln -s librjmcmc.0.dylib librjmcmc.dylib; }; })
libtool: install: /usr/bin/install -c .libs/librjmcmc.lai /usr/local/lib/librjmcmc.la
libtool: install: /usr/bin/install -c .libs/librjmcmc.a /usr/local/lib/librjmcmc.a
libtool: install: chmod 644 /usr/local/lib/librjmcmc.a
libtool: install: ranlib /usr/local/lib/librjmcmc.a
make[2]: Nothing to be done for `install-data-am'.
Making install in include
make[2]: Nothing to be done for `install-exec-am'.
 .././install-sh -c -d '/usr/local/include'
 .././install-sh -c -d '/usr/local/include/rjmcmc'
 /usr/bin/install -c -m 644  rjmcmc/bbox2d.h rjmcmc/curvefit.h rjmcmc/dataset1d.h rjmcmc/d
ataset2d.h rjmcmc/delaunay2d.h rjmcmc/engine.h rjmcmc/forwardmodel.h rjmcmc/forwardmodel_f
.h rjmcmc/forwardmodel_mpi.h rjmcmc/forwardmodelparameter.h rjmcmc/forwardmodel_util.h rjm
cmc/part1d_forwardmodel.h rjmcmc/part1d_natural_rj.h rjmcmc/part1d_regression_rj.h rjmcmc/
part1d_zero.h rjmcmc/part2d_forwardmodel.h rjmcmc/part2d_regression_rj.h rjmcmc/position_m
ap1d.h rjmcmc/position_map2d.h rjmcmc/position_map2d_delaunay.h rjmcmc/position_map2d_line
ar.h rjmcmc/position_map2d_quadtree.h rjmcmc/quadtree.h rjmcmc/regression.h rjmcmc/regress
ion_mpi.h rjmcmc/resultset1dfm.h rjmcmc/resultset1d.h rjmcmc/resultset2dfm.h rjmcmc/result
set2d.h rjmcmc/resultsetfm.h rjmcmc/rjmcmc_config.h rjmcmc/rjmcmc.h rjmcmc/rjmcmcf.h rjmcm
c/rjmcmcf_mpi.h rjmcmc/rjmcmc_debug.h rjmcmc/rjmcmc_defines.h rjmcmc/rjmcmc_random.h rjmcm
c/rjmcmc_util.h rjmcmc/single1d_regression.h rjmcmc/single2d_regression.h '/usr/local/incl
ude/rjmcmc'
 .././install-sh -c -d '/usr/local/include/rjmcmc'
 /usr/bin/install -c -m 644  rjmcmc/voronoi2d.h rjmcmc/wellrng.h '/usr/local/include/rjmcm
c'
make[2]: Nothing to be done for `install-exec-am'.
 ./install-sh -c -d '/usr/local/lib/pkgconfig'
 /usr/bin/install -c -m 644 rjmcmc.pc '/usr/local/lib/pkgconfig'
```

Figure 1: Terminal screenshot at the end of the installation of RJMCMC. The path to the installation folder is highlighted in light blue.

The way in which REDBACK deals with the temporal series of rotated angles deserves some further explanation. As mentioned, changes in angular velocity correspond to changes in the slope of the temporal series of rotated angle. This means that a constant angular velocity through time corresponds to a linear increase of the rotated angle, going backward in time. In order to better detect slope variations, REDBACK initially subtracts from the series of rotated angles the best–fitting linear regression profile, computed using the *weighted linear least squares* method. The result is a temporal series that accentuates changes of slopes, rather than actual angle values. We will refer to such a temporal series as *de–trended angle*. REDBACK applies trans–dimensional hierarchical Bayesian Inference to the de–trended angle and adds back the best–fitting linear trend initially subtracted, to obtain the noise–reduced temporal series of rotated angles.

4 Inputs to REDBACK

REDBACK needs two input files in order to run. The first one contains a set of temporally–consecutive finite rotations between two adjacent tectonic plates, from which noise will be reduced. The second one contains values for the simulation parameters (see Section 5.1 for details). These files may be stored anywhere on your machine.

4.1 Finite rotations file

Finite rotations of adjacent tectonic plates allow reconstructing their relative paleo–position at some time in the geological past [e.g. *Chang*, 1988]. Finite rotations represent 3D rigid rotations on a sphere. As such, their mathematical expression corresponds to 3x3 matrices. However, it is common practice within the Earth Sciences community to express them as three scalar values: latitude / longitude of the geographical location where the rotation axis intersects Earth' surface (also referred to as rotation pole), and angle that has been rotated about such an axis from the time associated with a particular inversion

```
7.8100000e-01   1.3720000e+02   6.6890000e+01   1.9600000e-01   1.4100000e-07  -7.4000000e-08   2.4700000e-07   4.2000000e-08  -1.3000000e-07   4.8200000e-07
1.7780000e+00   1.3879000e+02   6.2200000e+01   3.8500000e-01   8.7000000e-08  -4.5000000e-08   1.6500000e-07   3.5000000e-08  -7.8000000e-08   3.4500000e-07
2.5810000e+00   1.3744000e+02   6.3630000e+01   5.5900000e-01   4.9000000e-08   6.0000000e-09   5.1000000e-08   5.1000000e-08  -7.7000000e-08   2.1100000e-07
3.5960000e+00   1.3900000e+02   6.1840000e+01   7.6100000e-01   1.8900000e-07   2.2000000e-08   1.7400000e-07   1.0800000e-07  -1.0700000e-07   3.5900000e-07
4.1870000e+00   1.3581000e+02   6.3830000e+01   8.9200000e-01   3.0400000e-07   1.3000000e-08   2.5000000e-07   1.0800000e-07  -1.7100000e-07   5.6400000e-07
5.2350000e+00   1.3788000e+02   6.1100000e+01   1.0900000e+00   2.5800000e-07  -1.0000000e-08   3.2400000e-07   2.0100000e-07  -2.8400000e-07   8.5500000e-07
6.0330000e+00   1.3533000e+02   6.3290000e+01   1.2560000e+00   1.2700000e-07  -1.7000000e-08   1.7900000e-07   1.3000000e-07  -2.1300000e-07   5.7800000e-07
6.7330000e+00   1.3486000e+02   6.5730000e+01   1.4610000e+00   5.1700000e-07  -1.1500000e-07   7.7000000e-07   3.3400000e-07  -6.7500000e-07   2.0750000e-06
7.5280000e+00   1.3738000e+02   6.3210000e+01   1.5930000e+00   2.9500000e-07  -5.1000000e-08   4.3300000e-07   2.7100000e-07  -4.9200000e-07   1.3850000e-06
8.1080000e+00   1.3729000e+02   6.4430000e+01   1.7830000e+00   4.8500000e-07  -4.6000000e-08   5.9300000e-07   3.8200000e-07  -7.0400000e-07   1.9320000e-06
9.0980000e+00   1.3565000e+02   6.4860000e+01   2.0530000e+00   7.5800000e-07  -1.4600000e-07   1.0020000e-06   8.2900000e-07  -1.6050000e-06   3.9430000e-06
9.7790000e+00   1.3762000e+02   6.6100000e+01   2.2680000e+00   2.6460000e-06   4.2700000e-07   2.0050000e-06   1.1200000e-06  -1.2690000e-06   4.2160000e-06
1.1040000e+01   1.3317000e+02   6.7750000e+01   2.6220000e+00   8.1400000e-07  -1.2500000e-07   1.0010000e-06   5.3500000e-07  -1.0700000e-06   2.9800000e-06
1.2415000e+01   1.3386000e+02   6.7190000e+01   2.9880000e+00   9.2920000e-06   1.9000000e-07   8.3540000e-06   1.6970000e-06  -2.6090000e-06   1.2414000e-05
1.3734000e+01   1.3258000e+02   6.7390000e+01   3.3460000e+00   3.2556000e-05  -7.5640000e-06   4.3660000e-05   2.5400000e-06  -1.1419000e-05   6.0842000e-05
1.4581000e+01   1.2769000e+02   6.9500000e+01   3.6850000e+00   1.1925300e-04  -2.5358000e-05   1.5099300e-04   8.3870000e-06  -3.7123000e-05   2.0022700e-04
1.5974000e+01   1.3321000e+02   6.7970000e+01   4.0170000e+00   1.3687000e-05  -1.2090000e-06   1.4739000e-05   1.9830000e-06  -4.3130000e-06   2.0979000e-05
1.7235000e+01   1.2975000e+02   6.8850000e+01   4.3860000e+00   1.0038000e-05  -1.2950000e-06   1.2696000e-05   7.5900000e-07  -2.4000000e-06   1.7165000e-05
1.8056000e+01   1.2910000e+02   7.0160000e+01   4.7080000e+00   1.2383000e-05  -3.2690000e-06   1.7833000e-05   1.1630000e-06  -5.1810000e-06   2.6560000e-05
1.8748000e+01   1.2670000e+02   7.2120000e+01   5.0480000e+00   3.4083000e-05  -1.8520000e-06   4.1694000e-05   4.7560000e-06  -7.1720000e-06   5.6655000e-05
1.9722000e+01   1.3176000e+02   6.8620000e+01   5.0290000e+00   6.1630000e-06  -7.4200000e-07   7.1700000e-06   5.0800000e-07  -1.5630000e-06   9.6420000e-06
```

Figure 2: Example of how to format a set of temporally–consecutive finite rotations into a file to input to REDBACK. This example is shows the data set of *Merkouriev and DeMets* [2008, Table 2] for the relative paleo–position of Eurasia with respect to North America since ∼20 Ma.

of Earth's magnetic field in the geological past, to the present–day [e.g. *Cox and Hart*, 1986]. Such a time may be identified with the inversion name, as well as in Myr before the present–day – using a geomagnetic polarity reversal time–scale [e.g. *Cande and Kent*, 1995; *Lourens et al.*, 2004]. Scalar values of latitude, longitude and rotated angle are of course enough to build the associated 3x3 rotation matrix, should one wish to do so. The convention is that the axes $\hat{x}$, $\hat{y}$ and $\hat{z}$ of the Cartesian orthonormal system – in which rotation matrices are expressed – are chosen so that they intersect Earth' surface respectively at (0°E,0°N), (90°E,0°N) and (90°N).

A finite rotation is typically accompanied by a covariance matrix C, which has dimensions of radians (rad) squared and which is, by its nature, symmetric – that is, C is fully determined by six scalar values C_{11}, C_{12}, C_{13}, C_{22}, C_{23} and C_{33}. Entries of C are useful to determine the confidence interval associated with the finite rotation. We refer to *Chang* [1988] and *Royer and Chang* [1991] for a general account on finite rotations and their covariances.

The history of relative motions between two adjacent plates over a certain interval of time is reconstructed from a set of temporally–consecutive finite rotations, via differentiation according to the algebra of rotation matrices. We refer to *Merkouriev and DeMets* [2008, Tables 1 and 2] for an example of such a set, from which the relative motion between the Eurasia and North America plates over the past ∼20 Myr is derived.

In order to input a set of finite rotations to REDBACK, you must first store it within a plain–text file. Within such a file, each row must correspond to a single finite rotations, beginning from the most recent one and finishing with the oldest one, in temporally–consecutive order. Further, each row shall contain ten scalar values, ordered and expressed as follows: (1) time, expressed in Myr before the present–day, to which the finite rotation refers to. (2–3) Longitude and latitude, expressed in degrees, of the rotation pole. Longitude values shall be in range −180 to +180 (negative and positive values are respectively west and east of the Greenwich Meridian). (4) Angle, expressed in degrees, rotated from the time at (1) until the present–day. Note that angle values need to be positive. If your finite rotations feature negative angles, you will first need to (i) convert them into positive and (ii) take the antipodal points of the associated poles as new rotation poles, before feeding them to REDBACK. (5–10) Entries of the covariance matrix C associated with the finite rotation, expressed in rad^2, order as follows: C_{11}, C_{12}, C_{13}, C_{22}, C_{23} and C_{33}. Figure 2 is a screenshot showing an example of how such a file shall be formatted. In the specific case, the file contains finite rotations from *Merkouriev and DeMets* [2008, Table 2] for the relative Eurasia/North America paleo–position from 0.781 Ma (first row) to 19.722 Ma (last row).

Along with REDBACK, we provide two already–formatted files that are ready for use. Upon installation, you will find such files within the folder `REDBACK/EXAMPLES/`. These are

```
EU_NA_MD_GJI_2008_FINITE_ROTATIONS.txt
IN_SO_MD_G3_2006_FINITE_ROTATIONS.txt
```

The first of them is the one shown in Figure 2. The second contains finite rotations from *Merkouriev and DeMets* [2006] for the relative paleo–position between the India and Somalia plates since ∼20 Ma.

4.2 Parameters file

Parameters for each simulation of REDBACK must be stored into a plain–text file consisting of a list of names, one for each parameter, followed by values to assign. Such a parameter file has extension `.nml` – short for namelist. Figure 3 shows an example of such a file, which you will find under `REDBACK/EXAMPLES/EXAMPLE_INPUT_FILE.nml`. From Figure 3, you can see that the parameter section begins with the string `&redbacksettings`, and ends with the symbol `/` at the last line. You can also see that comments begin with the character `!`, and may be placed at the beginning of a line, as well as anywhere within the line, to comment from that point on. The example in Figure 3 shows all the possible parameters you can, and should, assign when running REDBACK. Each of these is discussed in detail in Section 5.1. In the particular example of Figure 3, only `input_data_file` and `ensemble_size` are assigned; while the rest of the parameters is commented out, allowing for default values (coded into the REDBACK source) to be used.

5 Setting the parameters and running REDBACK

5.1 Parameters setting

Most of the parameters that you will need to set in REDBACK serve the purpose of optimising the effectiveness of sampling the posterior probability distribution function of models, given the data [see *Iaffaldano et al.*, 2014, for more details]. In addition, a few more parameters serve to point to the input data set, as well as to use a couple of options for the outputs of REDBACK. In the following, we explain in detail each of the parameters you can set, in the same order in which they appear in the exemplary file `REDBACK/EXAMPLES/EXAMPLE_INPUT_FILE.nml` and in Figure 3.

1. `input_data_file`: String value for the path to the data sets (see Section 4.1) to input to REDBACK. There is no default value, since this parameter is mandatory for you to set.

2. `input_time_file`: String value for the path to a plain–text file containing a column of times (in Myr before present–day) at which you would like the final solution to be re–sampled. You will find an example of such a file under `REDBACK/EXAMPLES/EXAMPLE_TIME_STAGES.txt`. This parameter is optional for you to set, but is particularly suited to combine solutions from multiple finite–rotation data sets to reconstruct, for instance, the relative convergence between subducting and overriding plates. Should you choose to use this option, output Euler vectors and finite rotations (see Section 6) will feature the temporal resolution you request, as opposed to the native resolution of the original finite–rotation data set. Alternatively, the native resolution of the data set will instead be used as default.

3. `output_prefix`: String value that you can set as prefix to the names of all output files (see Section 6 for default values).

4. `ensemble_size`: Numeric value for the number of models to be generated by REDBACK. The totality of these models is the ensemble that REDBACK uses to sample the posterior probability distribution. We recommend keeping this number on the order of 10^6 or more. The default value is 10^6.

5. `burn_in`: Numeric value for the number of initial models not to be considered when sampling the posterior probability distribution of the entire ensemble. Since REDBACK starts by generating an initial random model [see *Iaffaldano et al.*, 2014, for more details], it is likely that this, and the few ones subsequently generated, will belong to a sub–space of the ensemble where models are unlikely to be a faithful realisation of the truth, given the data. Therefore it makes sense to discard them. In the jargon of Bayesian Inference, this allows the Markov chain to converge [*Malinverno*, 2002]. We recommend that this value be some two orders of magnitude smaller than `ensemble_size`. The default value is 10^4.

6. `max_partitions`: Integer value for the maximum number of changes in the slope of the temporal series of rotated angle (please remember that REDBACK actually deals with de–trended angles), as well as longitude and latitude of the

```
!
! This is an example of the input file to REDBACK.
! It contains all the parameters that users need to input,
! and may be modified for use.
!
! Comment lines begin with an exclamation mark.
! Comments about particular parameters can be made inline, as shown below.
! Users may comment out parameters to use default values, set in the source.
!
&redbacksettings
!
  input_data_file = './EXAMPLES/IN_SO_MD_G3_2006_FINITE_ROTATIONS.txt'
!  input_time_file = './EXAMPLES/EXAMPLE_TIME_STAGES.txt'
!  output_prefix = 'RBK_'
!
  ensemble_size = 1000000
!  burn_in = 10000
!  max_partitions = 20
!
!  time_sigma = 1  !Example: this parameter is set to 1
!
!  lon_sigma = 1
!  lon_sigma_bd= 1
!
!  lat_sigma = 1
!  lat_sigma_bd = 1
!
!  ang_sigma = 0.1
!  ang_sigma_bd = 0.1
!
!  hp_lon_min = 0.1
!  hp_lon_max = 10
!  hp_lon_sigma = 1
!
!  hp_lat_min = 0.1
!  hp_lat_max = 10
!  hp_lat_sigma = 1
!
!  hp_ang_min = 0.1
!  hp_ang_max = 10
!  hp_ang_sigma = 1
/
```

Figure 3: Example of a parameters file to be input to REDBACK. Parameter values shown are the ones used by default.

finite–rotation pole. Effectively, this corresponds to the maximum number of plate–motion changes that you wish to allow into the ensemble models. Any number of changes, from none to `max_partitions`, has equal chances to be cast into the models. This means that the prior distribution of probability [See *Iaffaldano et al.*, 2014] is uniform between 0 and `max_partitions`. We recommend that you set this value equal to the number of Myr that the finite–rotation data set covers. For instance, if you use `EU_NA_MD_GJI_2008_FINITE_ROTATIONS.txt`, which you find in `/REDBACK/EXAMPLES/`, you could set `max_partitions` to 20. This is because there is evidence suggesting that plate motions take at least 1 Myr to change [e.g. *Iaffaldano*, 2014]. Since most of the recent finite–rotation data sets [e.g. *DeMets et al.*, 2005; *Merkouriev and DeMets*, 2008; *Bull et al.*, 2010] cover the past 20 Myr, the default value for this parameter is 20.

7. `time_sigma`: This parameter concerns options 2 and 3 among the five described in [*Iaffaldano et al.*, 2014]. It is the standard deviation used by REDBACK to draw either the modified finite–rotation time, when perturbing an existing one (option 2), or to add a new finite–rotation (option 3) to the previously–accepted model. For the same reasons illustrated in the description of `max_partitions`, the default value of `time_sigma` is 1. We recommend exploring this parameter in range 0.05 to 5.

8. `lon_sigma`: This parameter concerns option 1 among the five described in [*Iaffaldano et al.*, 2014]. It is the standard deviation used by REDBACK to draw the new longitude of the finite–rotation pole, when perturbing the previously–accepted model. Such a perturbation results in a change of the temporal series of stage Euler vectors. The default value is 1. As an indication, we suggest starting from values around of 1/10 of the range of longitude spanned by the specific finite–rotation data set. For instance, you could set `lon_sigma` to 1 if you use `EU_NA_MD_GJI_2008_FINITE_ROTATIONS.txt`.

9. `lon_sigma_bd`: This parameter concerns option 3 among the five described in [*Iaffaldano et al.*, 2014]. It is the standard deviation used by REDBACK to draw the longitude of the finite–rotation pole to add to the previously–accepted model. The default value is 1. As an indication, we suggest starting from values similar to `lon_sigma`.

10. `lat_sigma`: Conceptually similar to `lon_sigma`, but concerning the latitude of model finite rotations. The default value is 1. As an indication, we suggest starting from values around of 1/10 of the range of latitude spanned by the specific finite–rotation data set.

11. `lat_sigma_bd`: Conceptually similar to `lon_sigma_bd`, but concerning the latitude of model finite rotations. The default value is 1. As an indication, we suggest starting from values similar to `lat_sigma`.

12. `ang_sigma`: Conceptually similar to `lon_sigma`, but concerning the de–trended angle of model finite rotations. The default value is 0.1. As an indication, we suggest starting from values around of 1/10 of the range of de–trended angle spanned by the specific finite–rotation data set (for convenience, this is printed to the terminal screen – see Figure 4).

13. `ang_sigma_bd`: Conceptually similar to `lon_sigma_bd`, but concerning the de–trended angle of model finite rotations. The default value is 0.1. As an indication, we suggest starting from values similar to `ang_sigma`.

14. `hp_lon_min`: This parameter concerns option 5 among the five described in [*Iaffaldano et al.*, 2014]. It is minimum value that you wish REDBACK assign to the hierarchical parameter of the model finite–rotation longitude. We suggest to keep this value set to 0.1 (default value), as it is unlikely that nominal uncertainties on finite–rotation data sets have been overestimated by a factor 10.

15. `hp_lon_max`: This parameter concerns option 5 among the five described in [*Iaffaldano et al.*, 2014]. It is maximum value that you wish REDBACK assign to the hierarchical parameter of the model finite–rotation longitude. We suggest to keep this value set to 10 (default value), as it is unlikely that nominal uncertainties on finite–rotation data sets have been underestimated by more than a factor 10.

16. `hp_lon_sigma`: This parameter concerns option 5 among the five described in [*Iaffaldano et al.*, 2014]. It is standard deviation that REDBACK uses to draw new values of the hierarchical parameter of the model finite–rotation longitude, starting from the previously–accepted model. We suggest to start by setting this value to 1 (default value). In the example of Section 8 we provide an indication of how to modify it.

17. `hp_lat_min`: Conceptually similar to `hp_lon_min`, but concerning the latitude of model finite rotations. The default value is 0.1.

18. `hp_lat_max`: Conceptually similar to `hp_lon_max`, but concerning the latitude of model finite rotations. The default value is 10.

19. `hp_lat_sigma`: Conceptually similar to `hp_lon_sigma`, but concerning the latitude of model finite rotations. The default value is 1.

20. `hp_ang_min`: Conceptually similar to `hp_lon_min`, but concerning the rotated angle of model finite rotations. The default value is 0.1.

21. `hp_ang_max`: Conceptually similar to `hp_lon_max`, but concerning the rotated angle of model finite rotations. The default value is 10.

22. `hp_ang_sigma`: Conceptually similar to `hp_lon_sigma`, but concerning the rotated angle of model finite rotations. The default value is 1.

5.2 Running REDBACK

Once you set the parameter values, or choose to use the default ones, you can run the executable REDBACK via a terminal. Move to the folder where REDBACK is located, and type the following command:

```
./REDBACK -n 'PATH TO PARAMETER FILE'
```

The option `-n`, which is the one we recommend, implies that you are using a namelist file. For instance, should you wish to use the examplary parameter file we provide along with REDBACK, you need to type

```
./REDBACK -n ./EXAMPLES/EXAMPLE_INPUT_FILE.nml
```

You also have the option of typing directly into the command line the path to the data set you wish to input to REDBACK. This is achieved by typing

```
./REDBACK -d 'PATH TO DATA SET FILE'
```

The option `-d` implies that you are using directly a file containing the finite–rotation data set. Note, however, that in such an instance, default values will be used for all the parameters. For instance, should you wish to use the finite rotations of *Merkouriev and DeMets* [2008] provided in the `EXAMPLE` folder, you need to type

```
./REDBACK -d ./EXAMPLES/EU_NA_MD_GJI_2008_FINITE_ROTATIONS.txt
```

Figure 4 is a terminal screenshot of a simulation performed using `EXAMPLES/EXAMPLE_INPUT_FILE.nml` as input. The data summary below the header reports data ranges that you could use to begin setting some of the parameters (see Section 5.1). An indication of the simulation progress is below the data summary.

```
============================================================
I                          REDBACK                         I
I                                                          I
I  REDBACK is an open-source software that implements the  I
I  trans-dimensional hierarchical Bayesian inference to    I
I  efficiently reduce the impact of finite-rotation noise  I
I  in plate-motion reconstructions.                        I
I                                                          I
I  REDBACK has been developed at the Research School of    I
I  Earth Sciences of the Australian National University    I
I  by                                                      I
I                                                          I
I  Rhys Hawkins                                           I
I  Giampiero Iaffaldano                                   I
I  Thomas Bodin                                           I
I  Malcolm Sambridge                                      I
I                                                          I
I  Canberra, February 2014                                 I
============================================================

Data Summary
            Data Points:  21
             Time Range:   0.781  19.722
        Longitude Range: 126.700 139.000
         Latitude Range:  61.100  72.120
            Angle Range:   0.196   5.048
 Angle de-trended Range:  -0.099   0.837
     Mean Lon/Lat/Angle: 134.384  66.031   2.387

 40% Completed
```

Figure 4: Terminal screenshot of a simulation in progress.

Figure 5 is a terminal screenshot of the completed simulation in Figure 4. At the end of each simulation, statistics on the models for finite–rotation pole and angle are reported. Columns correspond to the five options through which REDBACK perturbs a previously–accepted finite–rotation model, to generate the next one [*Iaffaldano et al.*, 2014]. The first value in each column is the number of models generated through a particular option among the five available. Note that the summation of these numbers equals the value of `ensemble_size`, and that the five options are more or less equally used to propose new models. The second value in each column is the number of proposed models, through a particular option among the five available, that REDBACK actually accepted to sample the posterior probability distribution. The third value in each column represents the percentage, or rate, of accepted models with respect to the proposed ones. As an indication, the total number of accepted models should be 30–60% of `ensemble_size` in order to ensure reasonable sampling of the model space. For instance, in the example in Figure 5, where default values have been used for all parameters, 38% and 14% of the proposed models for the temporal evolution of the finite–rotation pole and angle have been accepted. Tuning the simulation parameters, as we show in Section 8, helps improving the sampling effectiveness.

```
100% Completed

========= FINITE-ROTATION POLE ==========
              Birth     Death      Move     Value  Hierarch
Proposed:    400331    399581    400090    399738    400260
Accepted:     78693     78692    205313    256467    143183
Rate    :     19.66     19.69     51.32     64.16     35.77

========= FINITE-ROTATION ANGLE =========
              Birth     Death      Move     Value  Hierarch
Proposed:    399598    399934    400350    401226    398892
Accepted:     16038     16038    115088     37698     99595
Rate    :      4.01      4.01     28.75      9.40     24.97
```

Figure 5: Terminal screenshot of a completed simulation.

6 Outputs from REDBACK

REDBACK outputs thirteen plain–text files at the end of each simulation. These can be classified into three types: summary files, kinematic–output files and histogram files. The first and last types serve mainly the purpose of diagnostics, while kinematic–outputs are finite rotations and associated stage Euler vectors obtained upon reduction of noise. In the following, we explain in detail each of the files output by REDBACK:

1. `SUMMARY_input_finite_rotations.txt`: This is a copy of the finite–rotation data set provided in input. It features the same format of the input file.

2. `SUMMARY_parameter_values_used.txt`: This is a copy of the parameter file specified as input. It may be used again by simply changing its extension from `.txt` to `.nml`.

3. `SUMMARY_Euler_pole.txt`: This file contains the statistics shown in Figure 4 and Figure 5 related to the rotation pole. It also contains information such as date, time and simulation–duration.

4. `SUMMARY_Euler_angle.txt`: Conceptually similar to `SUMMARY_Euler_pole.txt`, but concerning the rotated angle.

5. `OUTPUT_FINITE_ROTATIONS.txt`: This file is one of the two kinematic–outputs from REDBACK. It contains the resulting finite rotations, upon reduction of noise. It is formatted exactly as the input finite rotations. If you provided a string value to `input_time_file` in the parameters file, then the output finite–rotation times will be those that you specified. Otherwise, they will be the same of the finite–rotation data set provided as input. Note that covariances associated with finite rotations are computed numerically, from the entire ensemble of accepted models, at the native resolution of the data set, or at the resolution that you specified using `input_time_file`.

6. `OUTPUT_EULER_VECTORS.txt`: This file is the other kinematic–output of REDBACK. It contains stage Euler vectors associated with `OUTPUT_FINITE_ROTATIONS.txt`. Each row corresponds to a single stage Euler vector, beginning from the most recent stage and ending with the oldest one, in temporally–consecutive order. Further, each row contains eleven scalar values, ordered and expressed as follows: (1–2) initial and final stage–time, expressed in Myr before the present–day. (3–5) $\hat{x}$, $\hat{y}$ and $\hat{z}$ components of the stage Euler vector, expressed in deg/Myr. (6–11) Entries of the covariance matrix ($\dot{C}$) associated with the stage Euler vector, expressed in $(\text{rad/Myr})^2$ and order as follows: $\dot{C}_{11}$, $\dot{C}_{12}$, $\dot{C}_{13}$, $\dot{C}_{22}$, $\dot{C}_{23}$ and $\dot{C}_{33}$. Note that $\dot{C}$ is not derived from `OUTPUT_FINITE_ROTATIONS.txt`, following the rule of propagation of uncertainties. Rather, they are computed numerically from the model ensemble. This effectively allows inferring more realistic values. The squared–root of columns 6, 9 and 11 have a particular meaning: If models were distributed normally around the average, then the squared–root of these columns would be the standard deviations associated with the $\hat{x}$, $\hat{y}$ and $\hat{z}$ components of the stage Euler vector, respectively. In this sense, such values provide an indication of how credible the solution provided by REDBACK is. For this reason, from here on we refer to them as *credible intervals*.

7. `HISTOGRAM_lon_hp.txt`: This file reports how frequently values for `hp_lon_sigma` within given intervals (or bins) have been accepted in the sampling process [see *Iaffaldano et al.*, 2014, for details]. It is made of two columns: the first contains mid–points of bins, the second contains the associated frequency counts. The width of bins is constant and equal to the difference between any two consecutive values within the first column. Plotting the second column against the first generates a histogram with the frequencies of values of `hp_lon_sigma`. If reasonable sampling of the model space has been achieved, plotted values are proportional to the probability density function of `hp_lon_sigma`.

8. `HISTOGRAM_lat_hp.txt`: Conceptually similar to `HISTOGRAM_lon_hp.txt`, but concerning `hp_lat_sigma`.

9. `HISTOGRAM_ang_hp.txt`: Conceptually similar to `HISTOGRAM_lon_hp.txt`, but concerning `hp_ang_sigma`.

10. `HISTOGRAM_num_Euler_angle_tchanges.txt`: This file reports how frequently a certain number of partitions, or slope changes, of the temporal series of rotated angle has been accepted across the ensemble of models. It is made of two columns: the first contains the number of partitions, the second contains the associated frequency counts. Plotting the second column against the first generates a histogram with the frequencies of number of changes cast into the rotated–angle model ensemble. If reasonable sampling of the model space has been achieved, plotted values are proportional to the probability density function of the partition number. It is worth reminding that the number of partitions of a model in fact corresponds to the number of plate–motion changes cast into the model.

11. `HISTOGRAM_Euler_angle_tchanges.txt`: This file reports how frequently a change in the temporal evolution of the rotated angle, occurring within a certain interval of time, has been accepted across the ensemble of models. It is made of two columns: the first contains mid–points of time intervals (or bins), the second contains the associated frequency counts. The width of bins is constant and equal to the difference between any two consecutive values within the first column. Plotting the second column against the first generates a histogram showing how frequently a change in the temporal series of rotated angle, occurring within a certain time interval, has been accepted. If reasonable sampling of the model space has been achieved, plotted values are proportional to the probability density function of the time of kinematic changes.

12. `HISTOGRAM_num_Epole_tchanges.txt`: Conceptually similar to `HISTOGRAM_num_Euler_angle_tchanges.txt`, but concerning the rotation pole.

13. `HISTOGRAM_Epole_tchanges.txt`: Conceptually similar to `HISTOGRAM_Euler_angle_tchanges.txt`, but concerning the rotation pole.

7 Post–simulation diagnostics

The output files from REDBACK can be used to generate a number of plots that serve as post–simulation diagnostics. These plots will help you to assess whether the choice of parameters yielded reasonable sampling of the model space; and to decide whether and how to refine parameter values.

If you are a MATLAB user, you are welcome to use the suite of `.m` files in `MATLAB_DIAGNOSTIC_SCRIPTS/` (located within the REDBACK folder). `REDBACKd_plotter.m` is the main function, while `REDBACKd_fr2ev.m`, `REDBACKd_rtm.m` and `REDBACKd_setup.m` are its dependancies. `REDBACKd_plotter.m` generates a `.eps` file containing a set of panels like those in Figure 6. You can get more information on each of the `.m` files (including the synopsis) by typing, in the MATLAB command window, `help` followed by the function name. If instead you prefer writing your own scripts for generating figures, then we suggest generating a suite of plots similar to the one in Figure 6.

Panels a–c are the components of stage Euler vectors along, respectively, the $\hat{x}$, $\hat{y}$ and $\hat{z}$ axes. In black are Euler–vector components obtained from the input finite rotations (the associated uncertainties are in grey), while in red is the solution, upon noise reduction, computed by REDBACK (credible intervals are in light red).

Panel d reports histograms for the recurrence of values of the hierarchical parameters across the ensemble of models, normalised to the maximum of each profile (i.e. a value of 1 means maximum occurrence). These are plots of the second against the first columns of `HISTOGRAM_lon_hp.txt` (in green), `HISTOGRAM_lat_hp.txt` (in blue) and `HISTOGRAM_ang_hp.txt` (in yellow). The peculiar shape of the three histograms, consisting of a smooth increase in the recurrence value, followed by a peak and a decrease to zero, is an indication that in this particular case reasonable sampling is very likely to have occurred.

Panel e reports histograms for the recurrence of values of the number of partitions across the ensemble of models, normalised to the maximum of each profile (i.e. a value of 1 means maximum occurrence). These plots report the second against the first columns of `HISTOGRAM_num_Epole_tchanges.txt` (in grey) and `HISTOGRAM_num_Euler_angle_tchanges.txt` (in black).

Panel f reports histograms for the recurrence of values of the times, within the interval spanned by input finite rotations, when temporal changes occur in the model ensemble. Histograms are normalised to the maximum of each profile (i.e. a value of 1 means maximum occurrence). These plots report the second against the first columns of `HISTOGRAM_Epole_tchanges.txt` (in grey) and `HISTOGRAM_Euler_angle_tchanges.txt` (in black).

Lastly, in addition to these diagnostic plots, we recommend keeping track of the acceptance rates for the model ensembles of finite–rotation angle and pole at the end of each calculation (see Figure 5). These will also be helpful in refining parameter values.

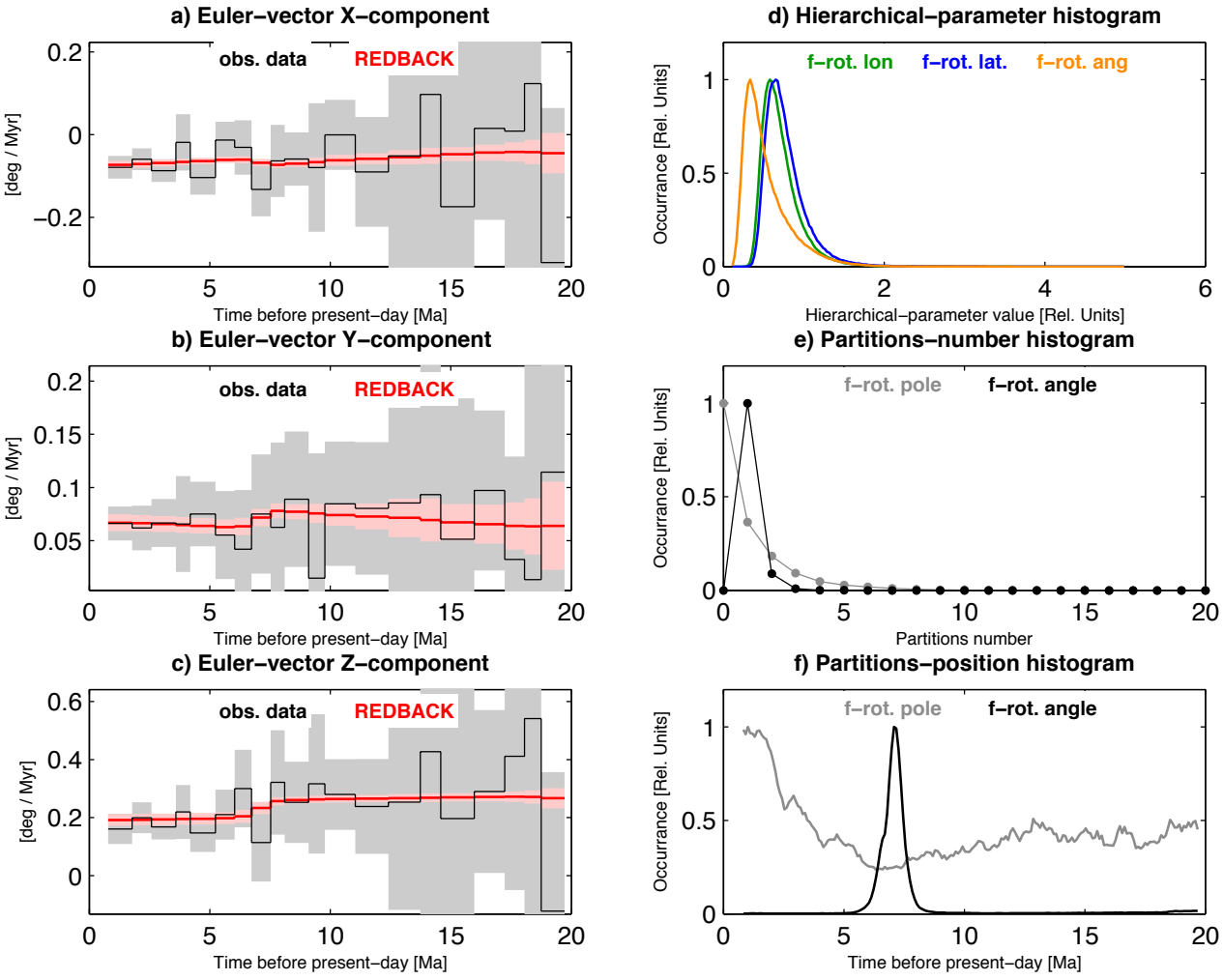

Figure 6: Example of diagnostic figures for REDBACK simulations.

8 An example of running REDBACK

In the following we propose an example of running REDBACK, using as input the data set of *Merkouriev and DeMets* [2008] for the relative paleo–position of Eurasia with respect to North America. You can find the associated finite–rotations file `EU_NA_MD_GJI_2008_FINITE_ROTATIONS.txt` in `EXAMPLES/`, inside the `REDBACK/` folder. This example has the explicit objective of showing how, in our opinion, parameter values should be set and refined in order to achieve reasonable sampling of the model space. It is worth reminding that, in theory, any choice of parameter values will, eventually, lead to reasonable sampling of the posterior [see *Iaffaldano et al.*, 2014, for more details]. In practice, however, you need to make sure that this is achieved within the number of iterations you set through the parameter `ensemble_size`.

8.1 Step 1

The first step we suggest you always take is running REDBACK with the default parameter values. This is readily achieved by commenting out most of the parameter declarations within the input `.nml` file. Figure 7 shows the result of doing so for `EU_NA_MD_GJI_2008_FINITE_ROTATIONS.txt`, while Figure 8 reports the associated statistics at the end of the calculation. The run–time of a calculation scales essentially with `ensemble_size`. This particular calculation, where `ensemble_size`=10^6, took ∼3 minutes of run–time on one 2.66 GHz processor with 8 GB of RAM.

As a general rule of thumb, obtaining (i) relatively smooth histograms for hierarchical parameters and partitions positions (like, for instance, those in Figure 6d and 6f), and (ii) acceptance rates in range 30–60% are good indications that reasonable sampling of the model space has been achieved within the number of iterations (i.e. `ensemble_size`). Furthermore, the extent of credible intervals (i.e. panels a–c in Figure 6) shall also be used as criterion for refining parameter values.

In Figure 7 it is clear, for instance, that histograms for the hierarchical parameters in panel d show increase, peak and then a relatively long coda. However, they are not as smooth as one may wish. Similarly, histograms in panel f suggest a kinematic change around 7 Ma, but smoothness may be improved. Lastly, the ensemble statistics (Figure 8) indicate that 36% of models of both rotated angle and rotation pole have been accepted. While this is acceptable, higher rates would be desirable.

Altogether, these indications do warrant refinement of the default input parameters. We suggest starting from the hierarchical parameters. The fact that histograms in panel d feature a relatively long coda indicates that the ranges of values explored were perhaps too wide, and may be reduced. At step 2 we decrease the values of `hp_ang_max`, `hp_lon_max` and `hp_lat_max` (see Section 5.1) from the default (10) to 6.

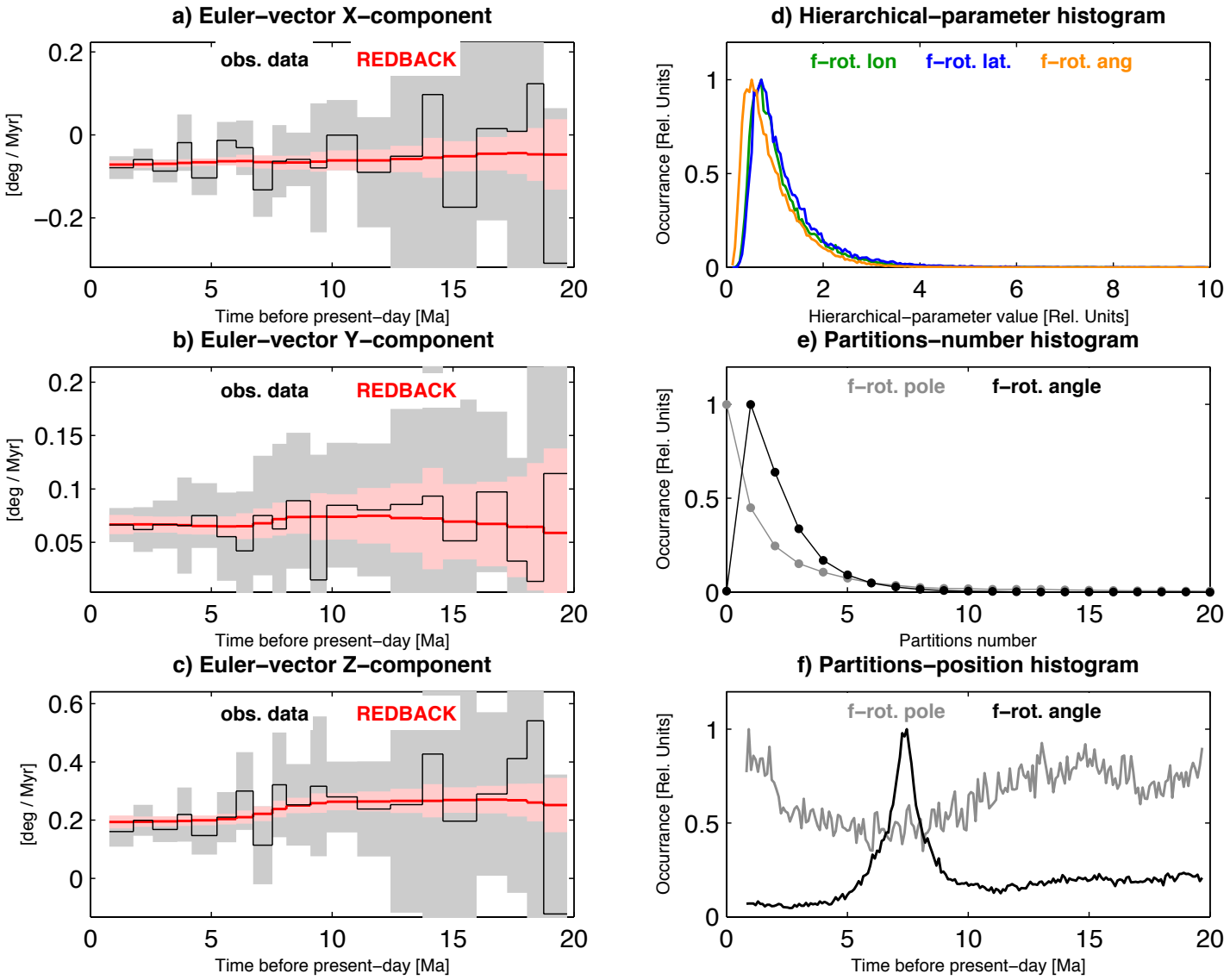

Figure 7: Diagnostics associated with step 1

```
========= FINITE-ROTATION POLE ==========
              Birth      Death       Move      Value  Hierarch
Proposed:    199782     199987     199492     200576    200163
Accepted:     25237      25237      86074     149521     72424
Rate    :     12.63      12.62      43.15      74.55     36.18

========= FINITE-ROTATION ANGLE =========
              Birth      Death       Move      Value  Hierarch
Proposed:    199718     200238     199963     200229    199852
Accepted:     43907      43906     123626      80433     65656
Rate    :     21.98      21.93      61.82      40.17     32.85
```

Figure 8: Ensemble statistics associated with step 1

8.2 Step 2

In Figure 9 we note that histograms for the hierarchical parameters are even less smooth than before. This typically indicates that values of the standard deviations with which they are perturbed, from one accepted model to the next (see description of perturbation–option 5 in *Iaffaldano et al.* [2014]), are somewhat high. In fact, if this is the case, the hierarchical parameter(s) will be perturbed towards values relatively far away from the previously–accepted one, preventing REDBACK from performing sufficient sampling in the vicinity of the latter – once again, within the pre–set number of iterations. By the same logic, if the standard deviation of the hierarchical parameter(s) is set to small values, sampling will occur predominantly in the vicinity of certain values, with little chance of moving away from them. The result is that histogram(s) would show pronounced peaks on such values, and almost no occurrence elsewhere. At step 3, therefore, we proceed by decreasing only `hp_ang_sigma` from the default value (1) to 0.5. In fact, we suggest refining standard deviations of hierarchical parameters one at a time.

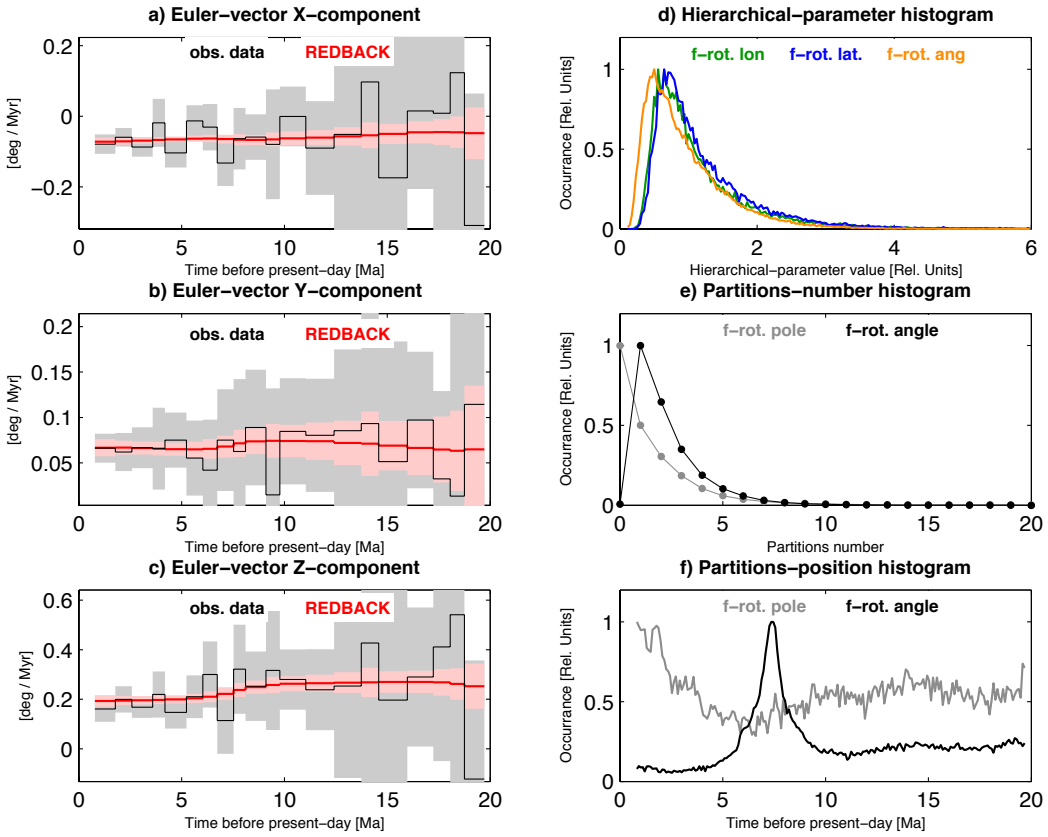

Figure 9: Diagnostics associated with step 2

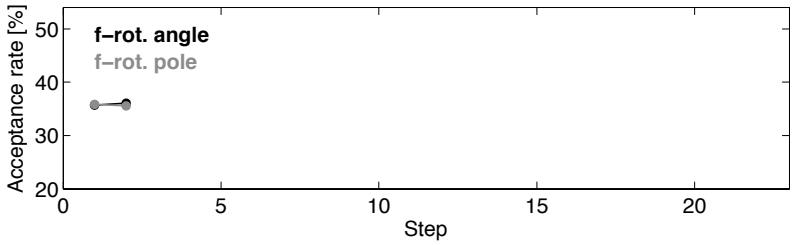

Figure 10: Progression of acceptance rates at step 2

8.3 Step 3

The histogram for the hierarchical parameter associated with the rotated angle (Figure 11d, in yellow) appears now smoother than before, suggesting that reasonable sampling has been achieved within the default number of iterations (10^6). However, we also note (i) a decrease of the acceptance rate of rotated–angle models (Figure 12, in black) and (ii) a moderate widening of the credible intervals – particularly those in Figure 11b. On this basis, it is worth testing whether even smaller values of `hp_ang_sigma` confirm this pattern. At step 4, therefore, we decrease further `hp_ang_sigma` from 0.5 to 0.1.

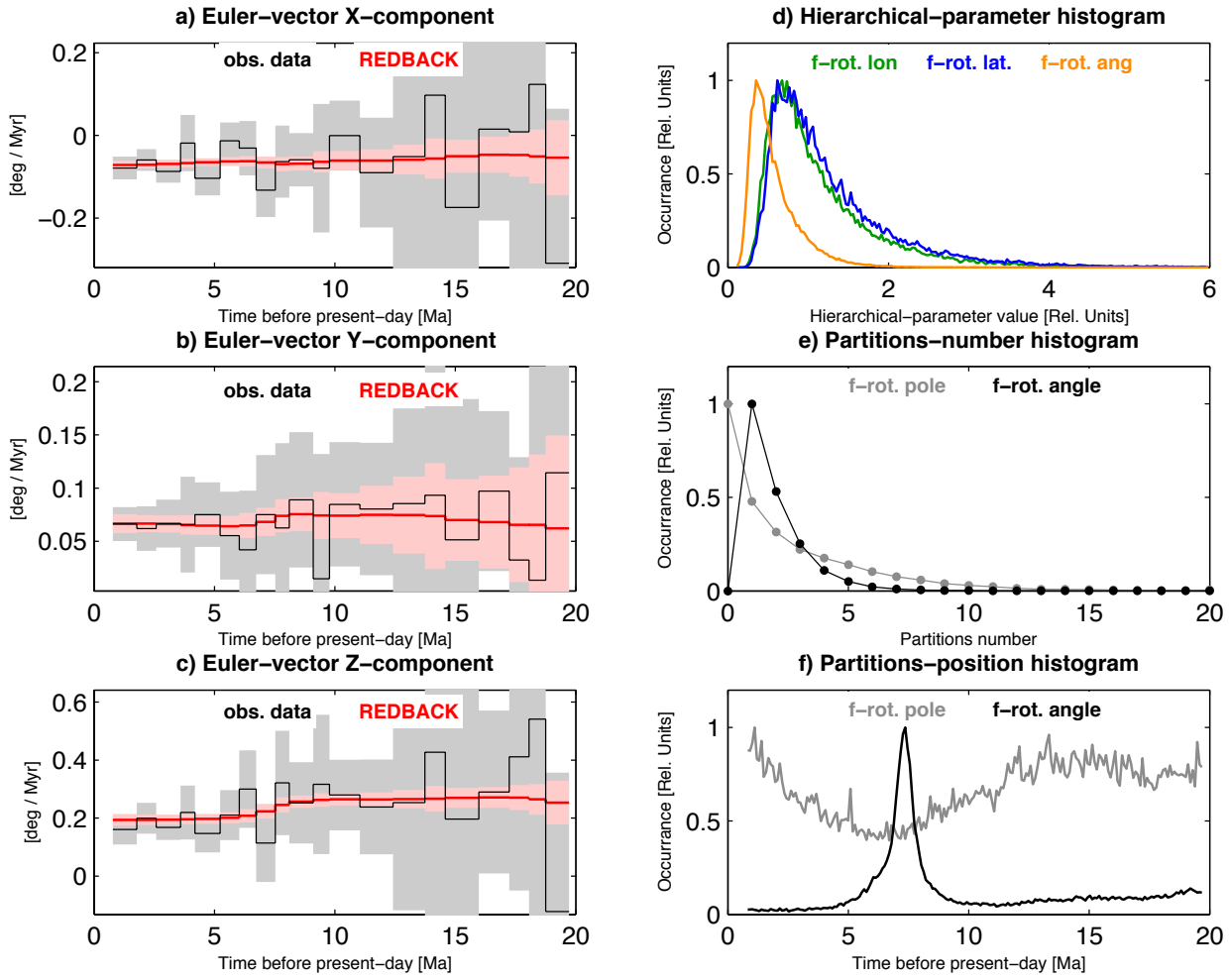

Figure 11: Diagnostics associated with step 3

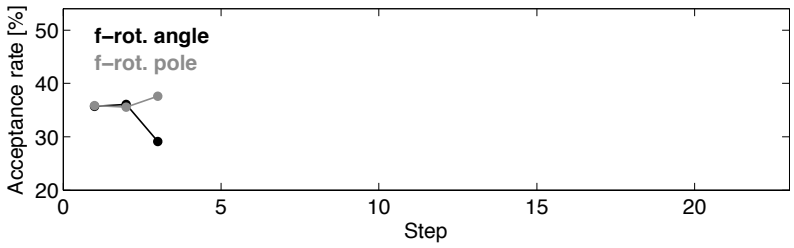

Figure 12: Progression of acceptance rates at step 3

8.4 Step 4

While Figure 13d shows a relatively smooth histogram of the hierarchical parameter for the rotated angle (yellow profile), we note from Figure 13f that the black profile now shows a second smaller, but distinct peak. We tend to deem this not a true feature of the kinematic time–series. Further, the acceptance rate for rotated–angle models has further decreased below the 30–60 % range. These observations indicate that `hp_ang_sigma` < 1 perhaps yields unreasonable sampling. Therefore, at step 5 we test the impact of increasing `hp_ang_sigma` to 2.

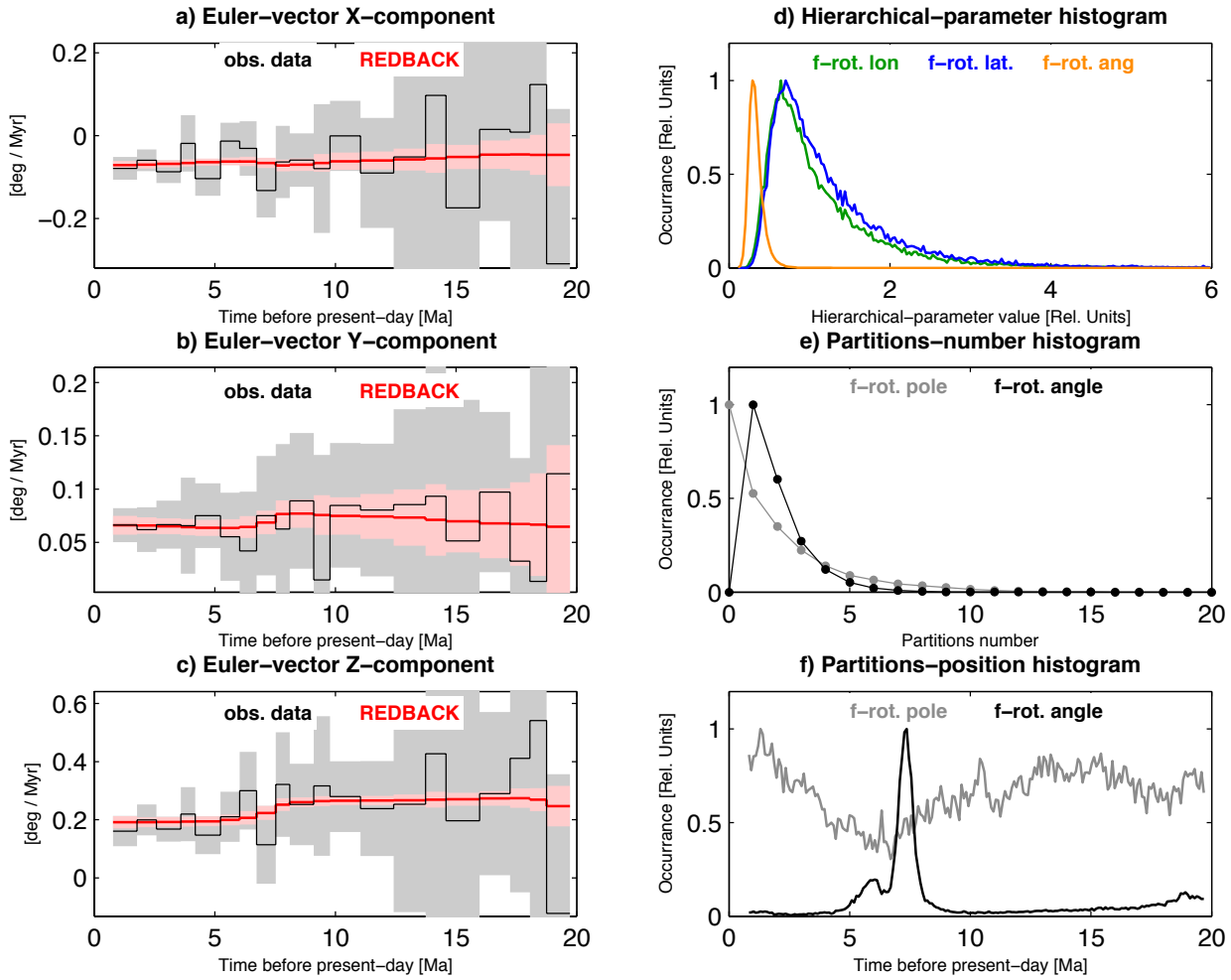

Figure 13: Diagnostics associated with step 4

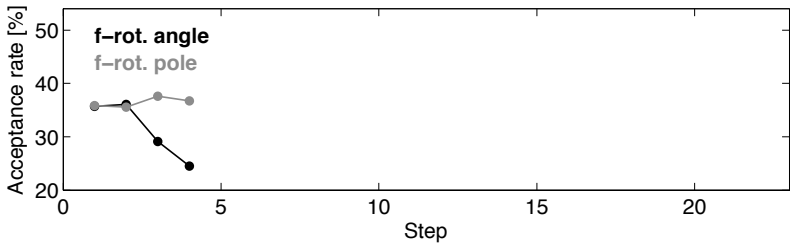

Figure 14: Progression of acceptance rates at step 4

8.5 Step 5

While the acceptance rate for rotated–angle models has now improved (Figure 16), the smoothness of the yellow profile in Figure 15d is not satisfactory. Note also a worsening of the histograms in Figure 15f. Nonetheless, to confirm this pattern, at step 6 we keep increasing `hp_ang_sigma` to 3.

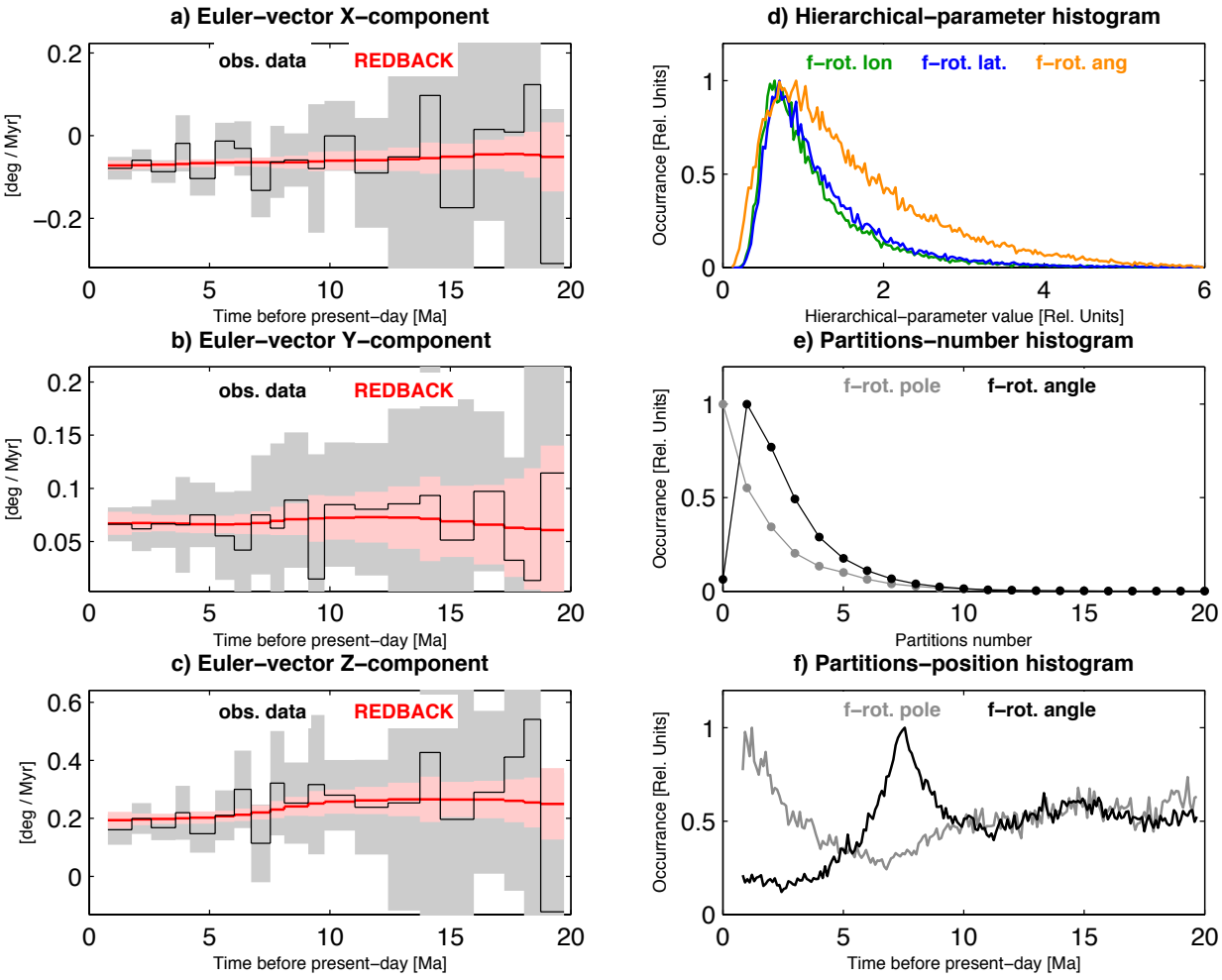

Figure 15: Diagnostics associated with step 5

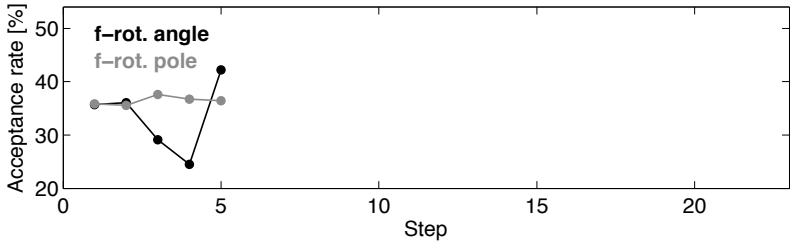

Figure 16: Progression of acceptance rates at step 5

8.6 Step 6

The acceptance rate for rotated–angle models Figures 18 is satisfactory, but panels d and f in Figures 17 clearly show a worsening of histograms. Widening of credible intervals is also observed (Figures 17a–c). From the results of steps 2–6 it appears that the ideal value of `hp_ang_sigma` must be at least 1, but smaller than 2. Therefore at step 7 we set `hp_ang_sigma` = 1.5.

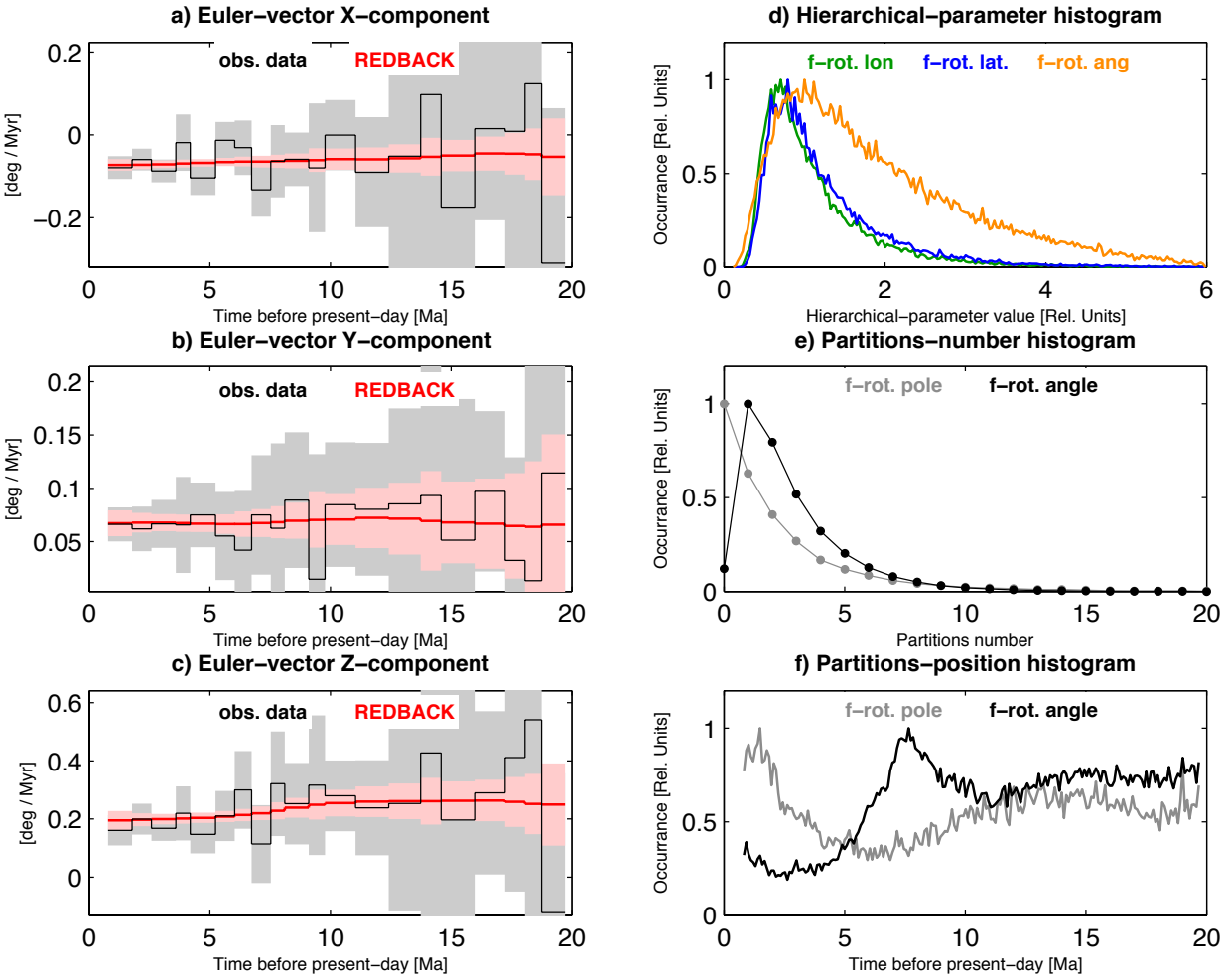

Figure 17: Diagnostics associated with step 6

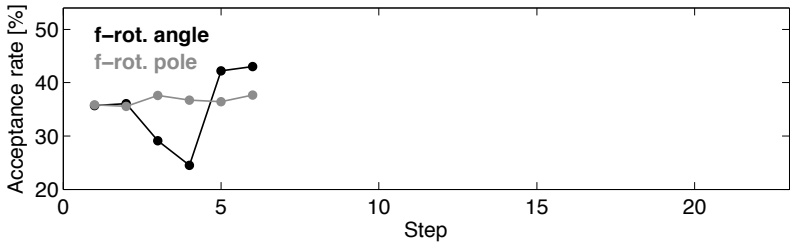

Figure 18: Progression of acceptance rates at step 6

8.7 Step 7

It appears that `hp_ang_sigma` = 1 (step 2, Figure 9) and `hp_ang_sigma` = 1.5 (step 7, Figure 19) yield the best results. Among the two, we decide to settle on `hp_ang_sigma` = 1 for the following reasons: (1) it yields a smoother hierarchical–parameter histogram, (2) it yields a clearer histogram for the partition–position, (3) the associated acceptance rate of rotated–angle models is anyways satisfactory and (4) the associated credible intervals are narrower. At the same time, at step 8 we begin modifying `hp_lon_sigma`. Having considered the green profile (associated with the time series of rotation–pole longitude) in Figure 9d (where `hp_ang_sigma` = 1), we begin by decreasing its value from the default (1) to 0.5.

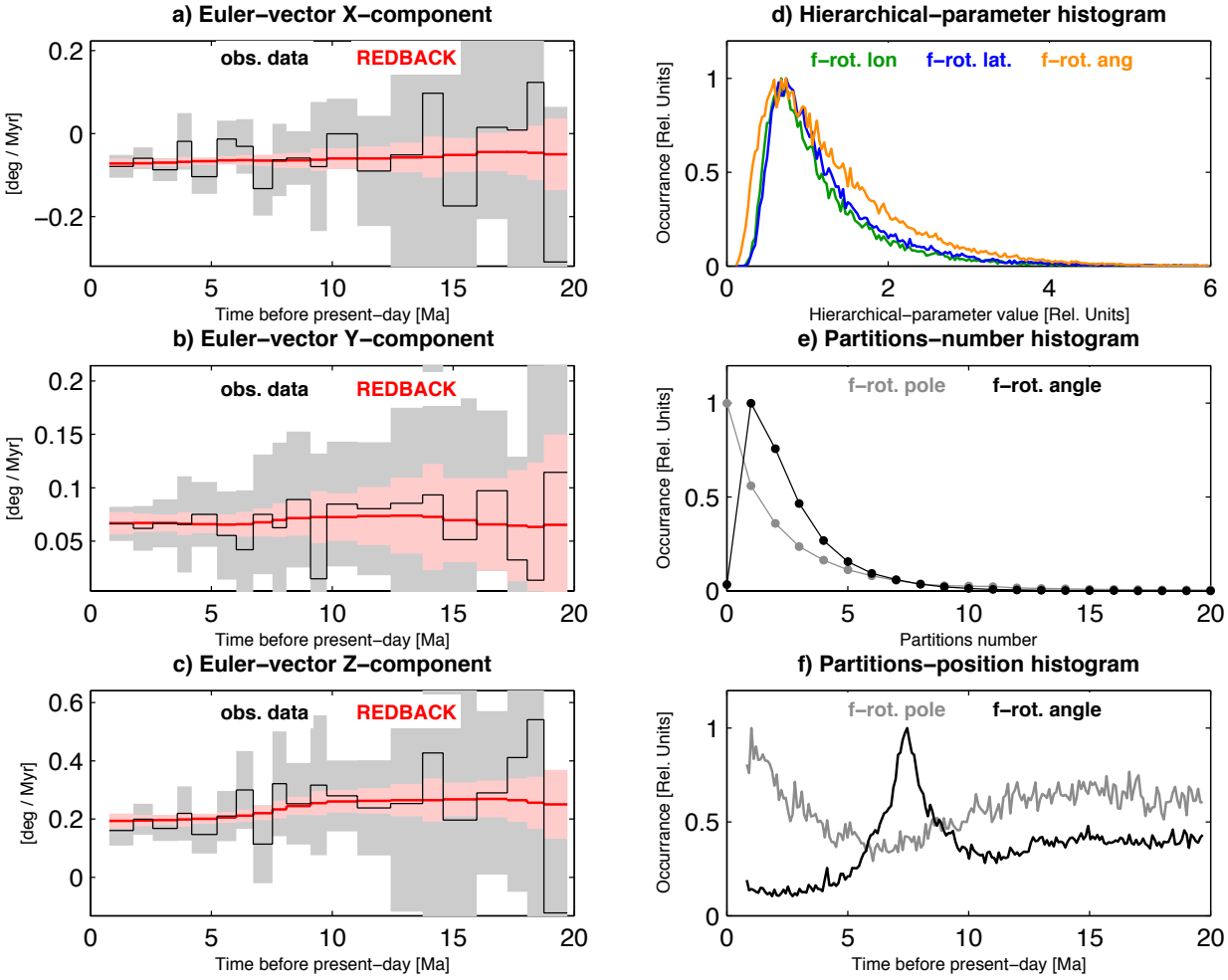

Figure 19: Diagnostics associated with step 7

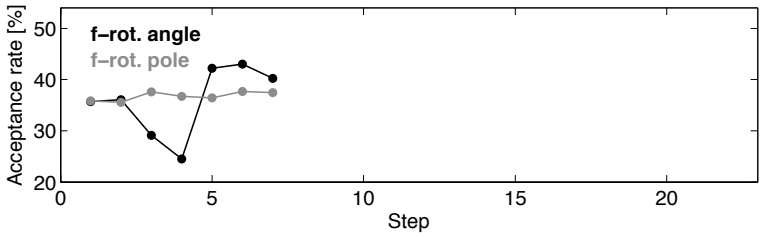

Figure 20: Progression of acceptance rates at step 7

8.8 Step 8

Decreasing `hp_lon_sigma` yields some improvement of the hierarchical–parameter histogram associated with the time series of rotation–pole latitude (Figure 21d) with respect to step 2 (which featured the same values for all other parameters). Further, the acceptance rate for rotation–pole models is effectively the same of step 2, while credible intervals are now slightly wider. We elect to test even lower values of `hp_lon_sigma`. At step 9 we decrease it to 0.1.

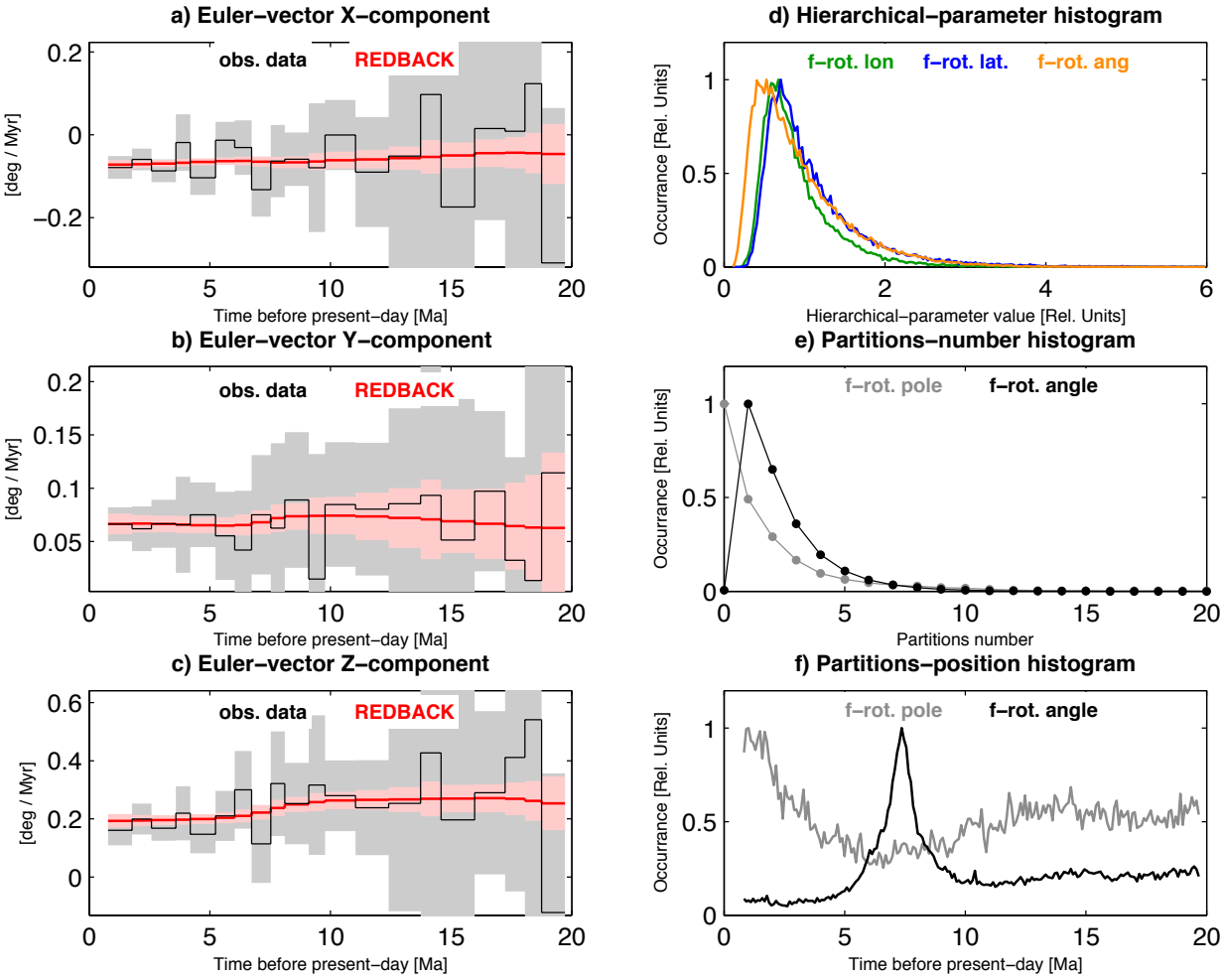

Figure 21: Diagnostics associated with step 8

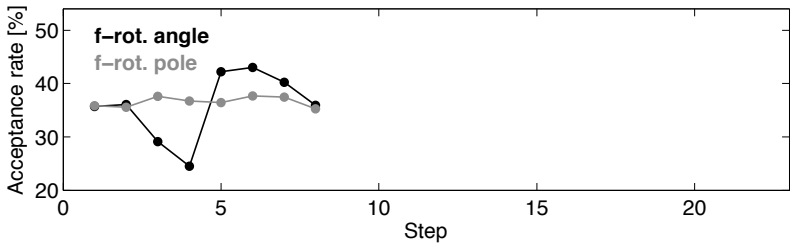

Figure 22: Progression of acceptance rates at step 8

8.9 Step 9

Overall, values of `hp_lon_sigma` smaller than 1 seem to yield more or less reasonable sampling. At step 10 we explore the effect of `hp_lon_sigma` > 1. Specifically, we set `hp_lon_sigma` $= 3$.

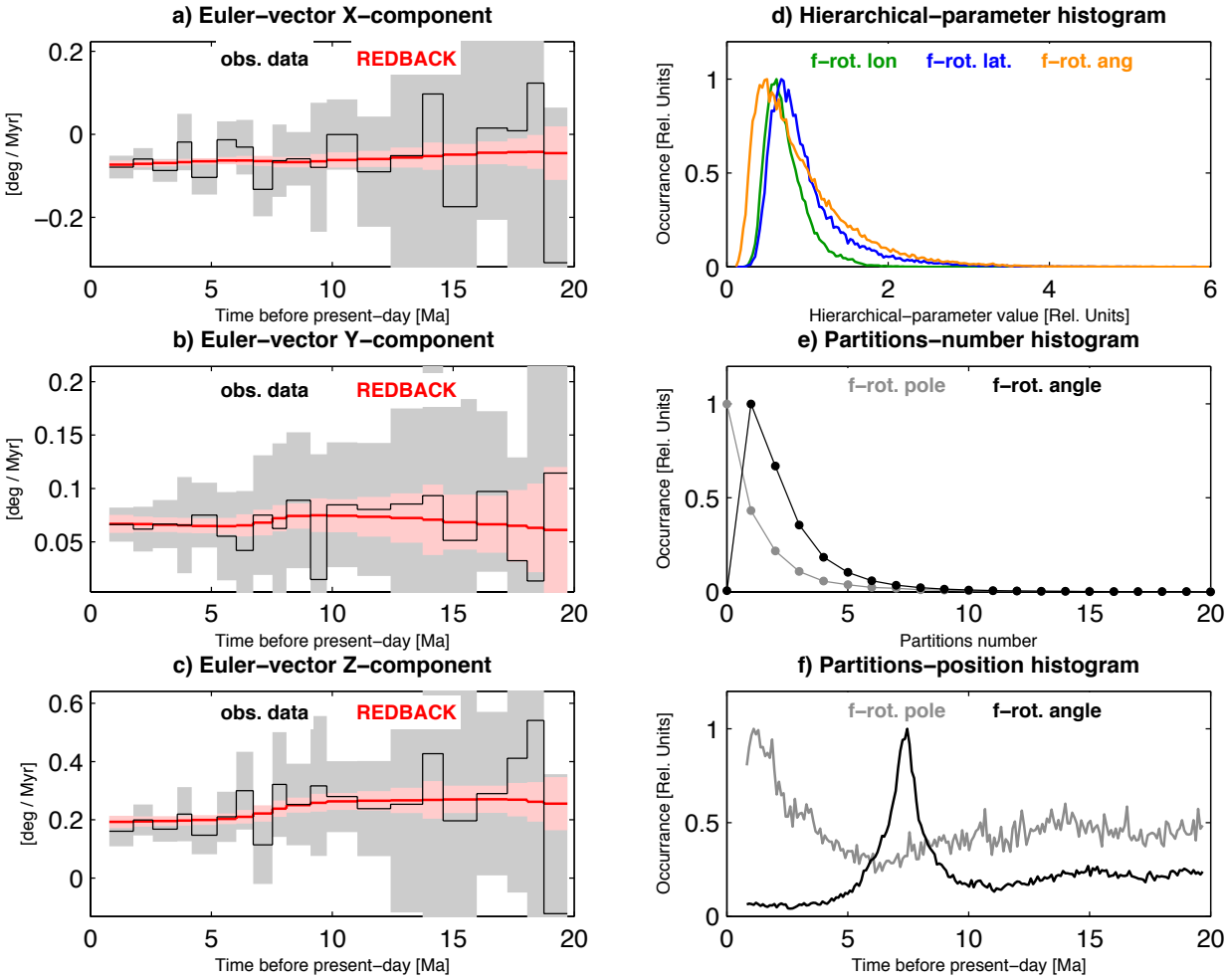

Figure 23: Diagnostics associated with step 9

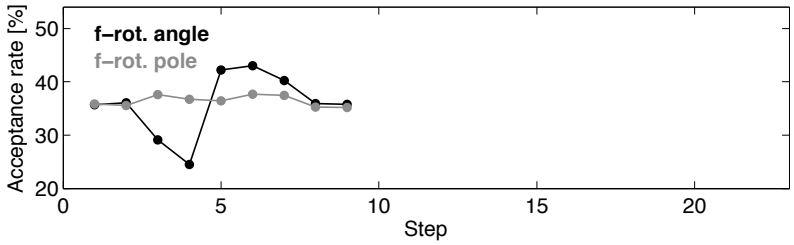

Figure 24: Progression of acceptance rates at step 9

8.10 Step 10

Setting `hp_lon_sigma` > 1 yields a clear worsening of the sampling quality. This is evident by comparing histograms and credible intervals in Figure 25 with those in Figures 23 or 9. At the same time, setting `hp_lon_sigma` > 1 yields an increase in the acceptance rate of rotation–pole models (grey profile in Figure 26). This may seem counter–intuitive, and requires some explanation: in general, acceptance rates indicate how many of the proposed models have been deemed a faithful realisation of the truth, given the data. However, they say nothing on whether the sampled region is wide enough to encompass (ideally) all possible models. A worsening of histograms of hierarchical parameters accompanied by an increased in acceptance rates may be explained by arguing that a small portion of the model space has been sampled (i.e. under–sampling occurred), but the quality of sampling in such a small portion is still satisfactory. This is, however, not satisfactory in general terms, as one should aim at reasonable sampling across (ideally) the entire model space. For these reasons, we decide to settle on `hp_lon_sigma` $= 0.1$, as it represents in our opinion the best compromise between acceptance rate for rotation–pole models, smoothness of histograms, and credible intervals of stage Euler vectors. Furthermore, at step 11 we begin refining `hp_lat_sigma`. We decrease its value from the default (1) to 0.5.

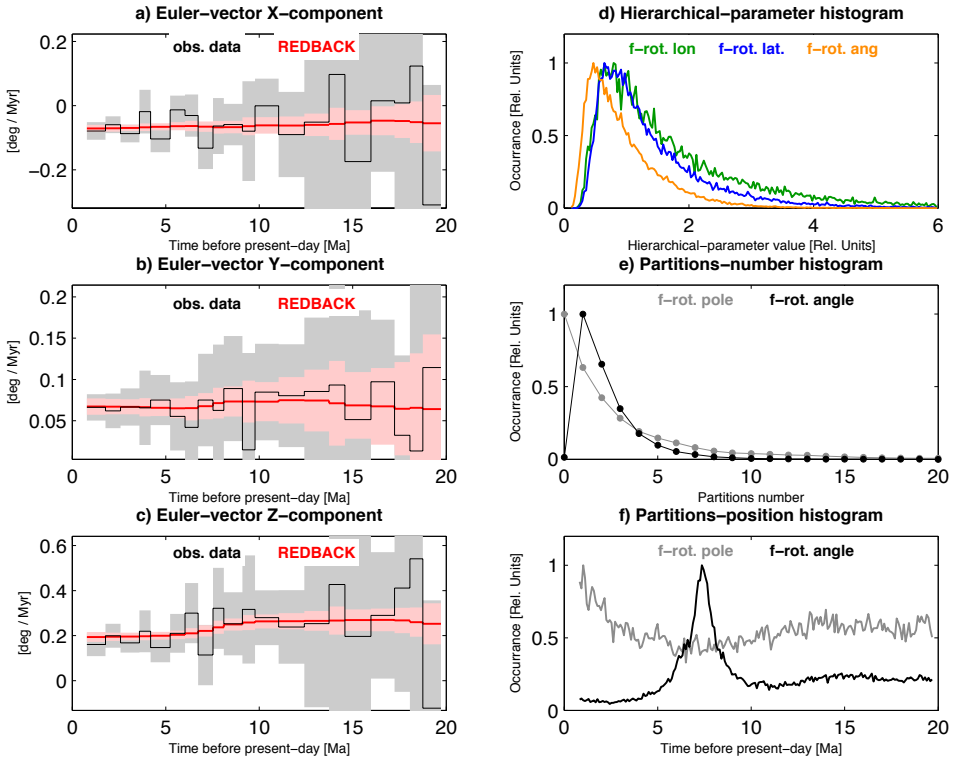

Figure 25: Diagnostics associated with step 10

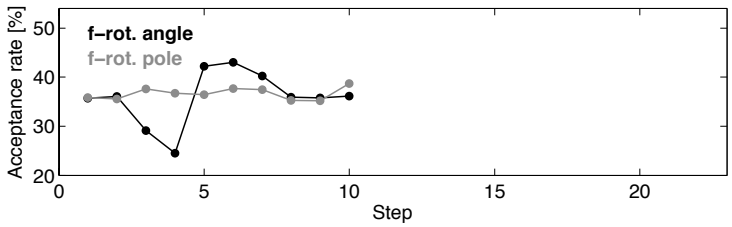

Figure 26: Progression of acceptance rates at step 10

8.11 Step 11

Setting `hp_lat_sigma` = 0.5 yields smoother histograms (Figure 27d, f) and narrower credible intervals (Figure 27a–c), while the acceptance rate of rotation–pole models remains similar to that associated with the default value. This suggests exploring the effect of even smaller values of `hp_lat_sigma`. At step 12 we keep decreasing it to 0.1.

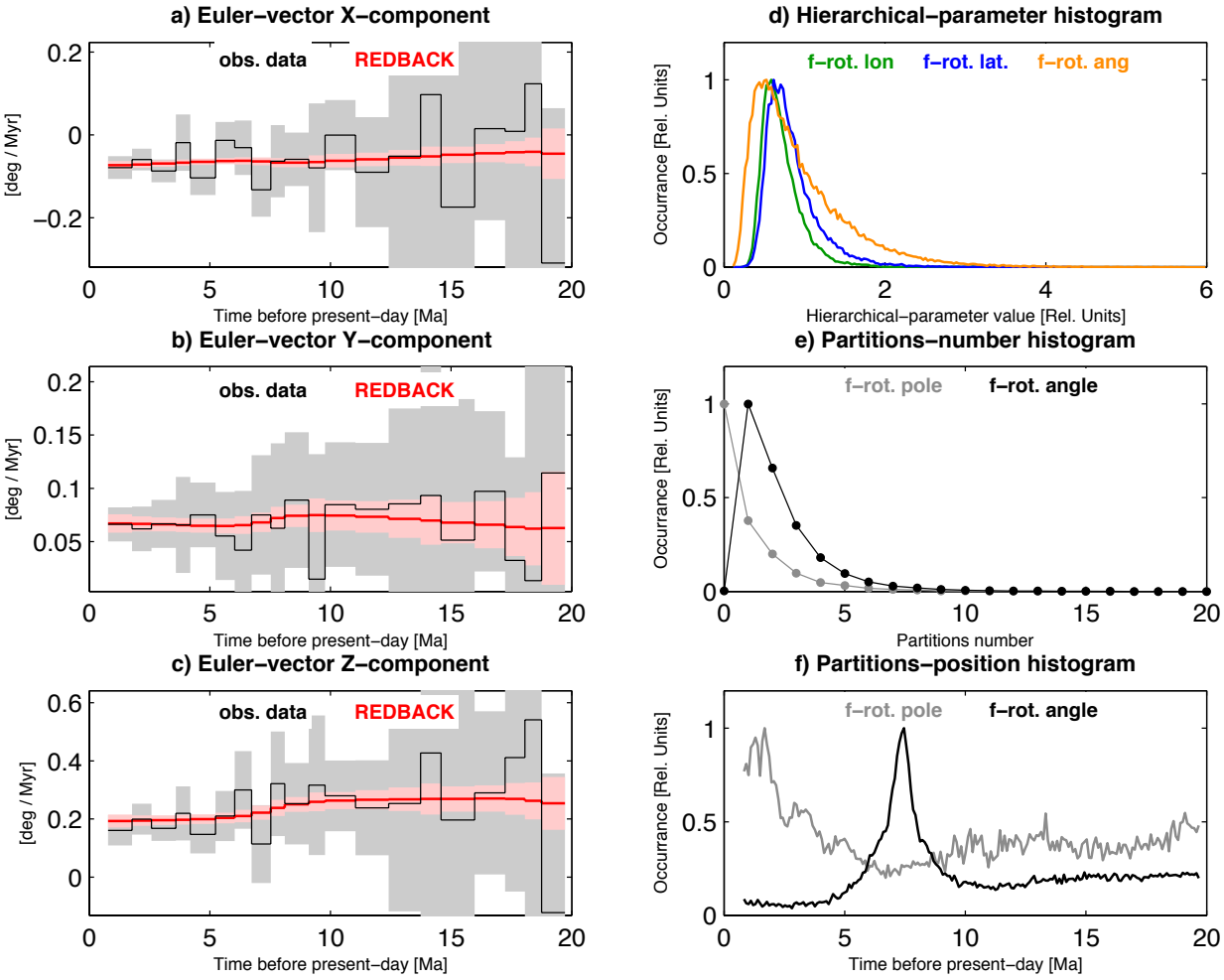

Figure 27: Diagnostics associated with step 11

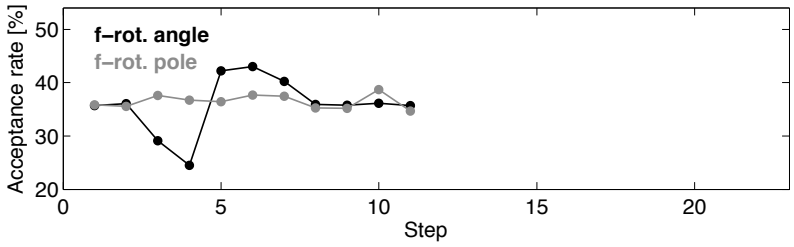

Figure 28: Progression of acceptance rates at step 11

8.12 Step 12

Considering the general improvement that is evident in Figures 29 and 30, at step 13 we decrease `hp_lat_sigma` further to 0.01.

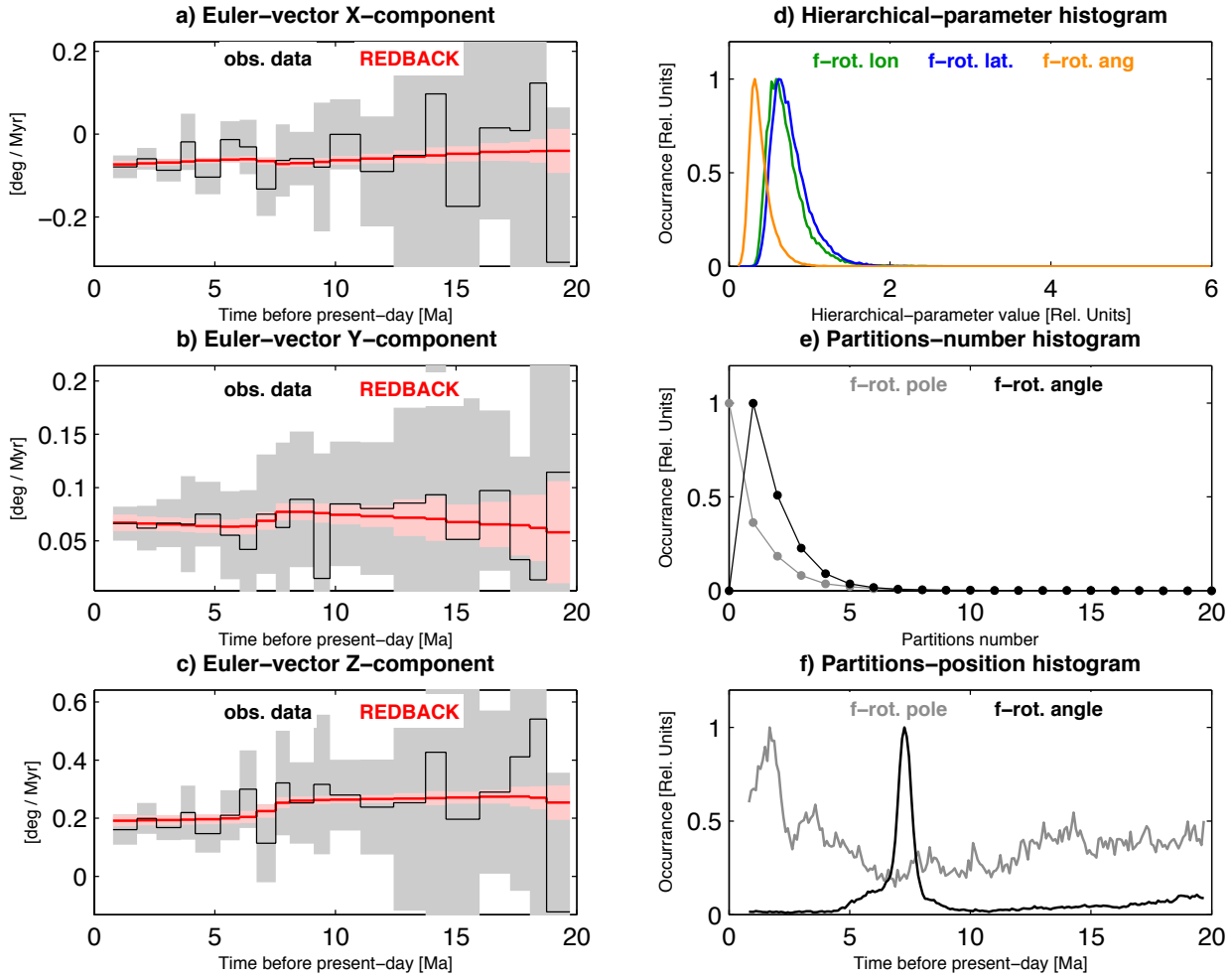

Figure 29: Diagnostics associated with step 12

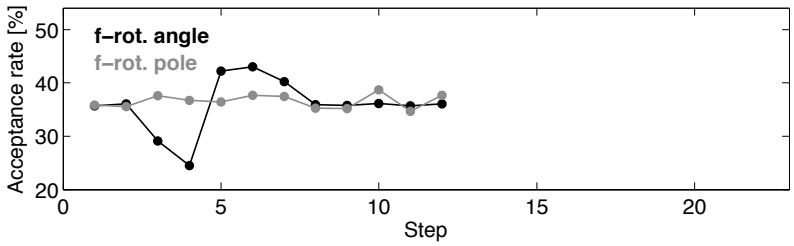

Figure 30: Progression of acceptance rates at step 12

8.13 Step 13

Setting `hp_lat_sigma` = 0.01 yields under–sampling, as evidenced by the hierarchical–parameter histogram in Figure 31 (blue profile). Note, once again, an increase in the acceptance rate of rotation–pole models (Figure 32, grey profile). This provides an even clearer example of the notion discussed at step 10: that under–sampling may be accompanied by an increase in acceptance rates, and that in general one needs to consider multiple indicators (histograms smoothness, credible intervals, acceptance rates), rather than just a single one at a time, in order to make a sensible choices of parameter values. At step 14 we explore the impact of setting `hp_lat_sigma` > 1. We set `hp_lat_sigma` = 3.

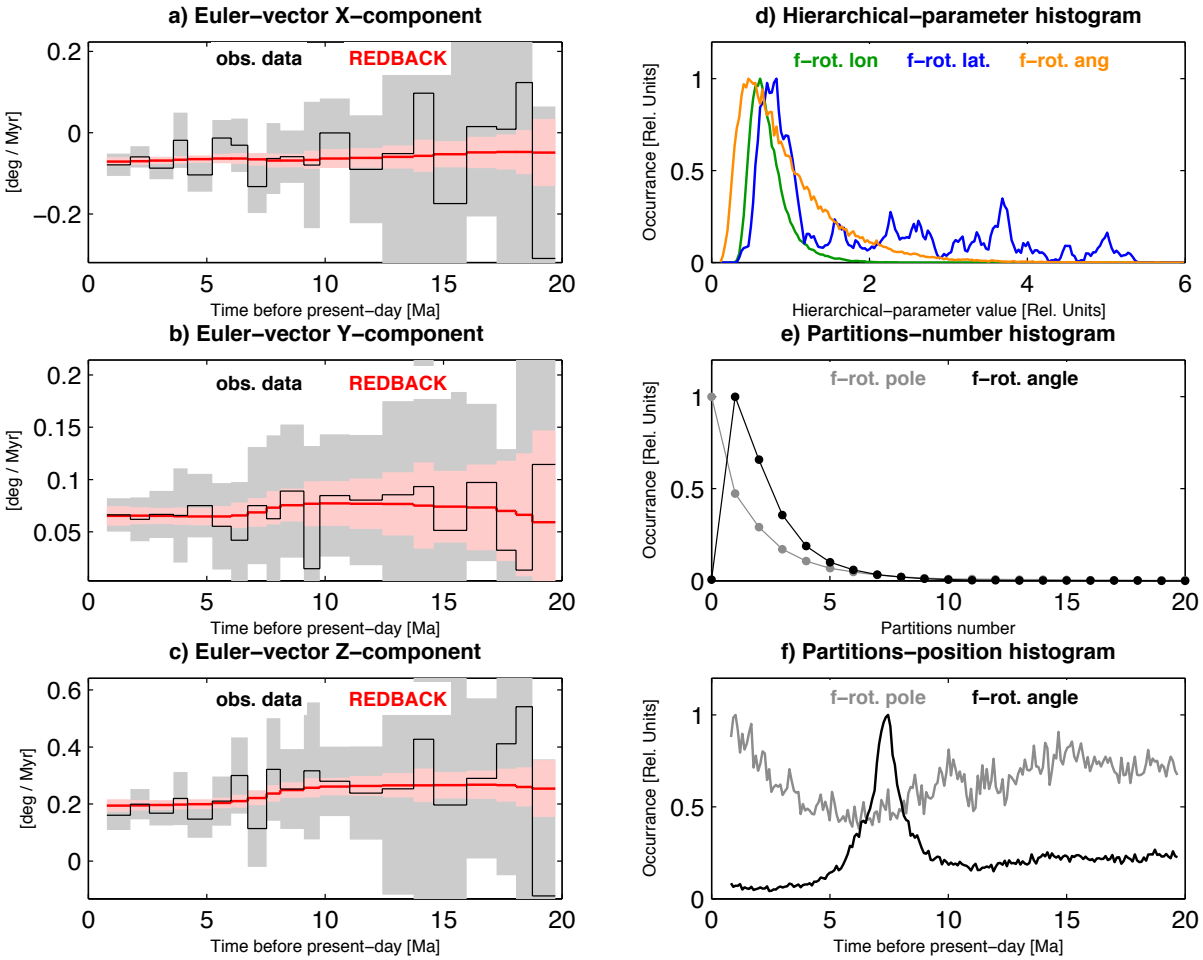

Figure 31: Diagnostics associated with step 13

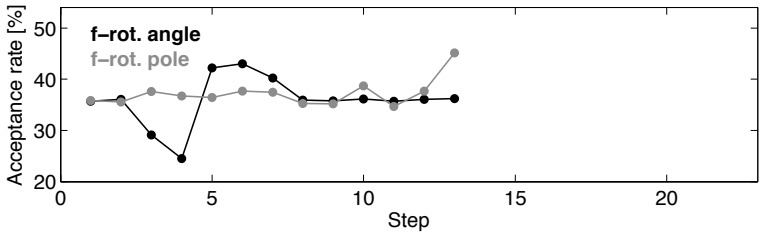

Figure 32: Progression of acceptance rates at step 13

8.14 Step 14

Setting `hp_lat_sigma` = 3 yields results that are not as good as those at step 12 in terms of histograms smoothness and credible intervals. Therefore at step 15 we settle on `hp_lat_sigma` = 0.1 (see Figure 29). One may argue that the shape of histograms in Figure 29d is satisfactory, but not ideal. While we could agree we such a statement, we shall keep in mind that some improvement in sampling will naturally occur simply by increasing the value of `ensemble_size`, which we suggest always doing as final step. In this sense, we consider the sampling of the hierarchical parameters satisfactory at this stage. Next, we suggest that you refine the value of `time_sigma` (see Section 5.1), which is used to implement perturbation–options 2 and 3 in *Iaffaldano et al.* [2014]. The impact of `time_sigma` is visible from the the histograms of partitions–positions in panel f. In order to refine `time_sigma`, we suggest to use the same rule of thumb used for the hierarchical parameters – that is, trying to obtain histograms as smooth as possible. At step 15, therefore, we proceed by decreasing `time_sigma` from the default value (1) to 0.1.

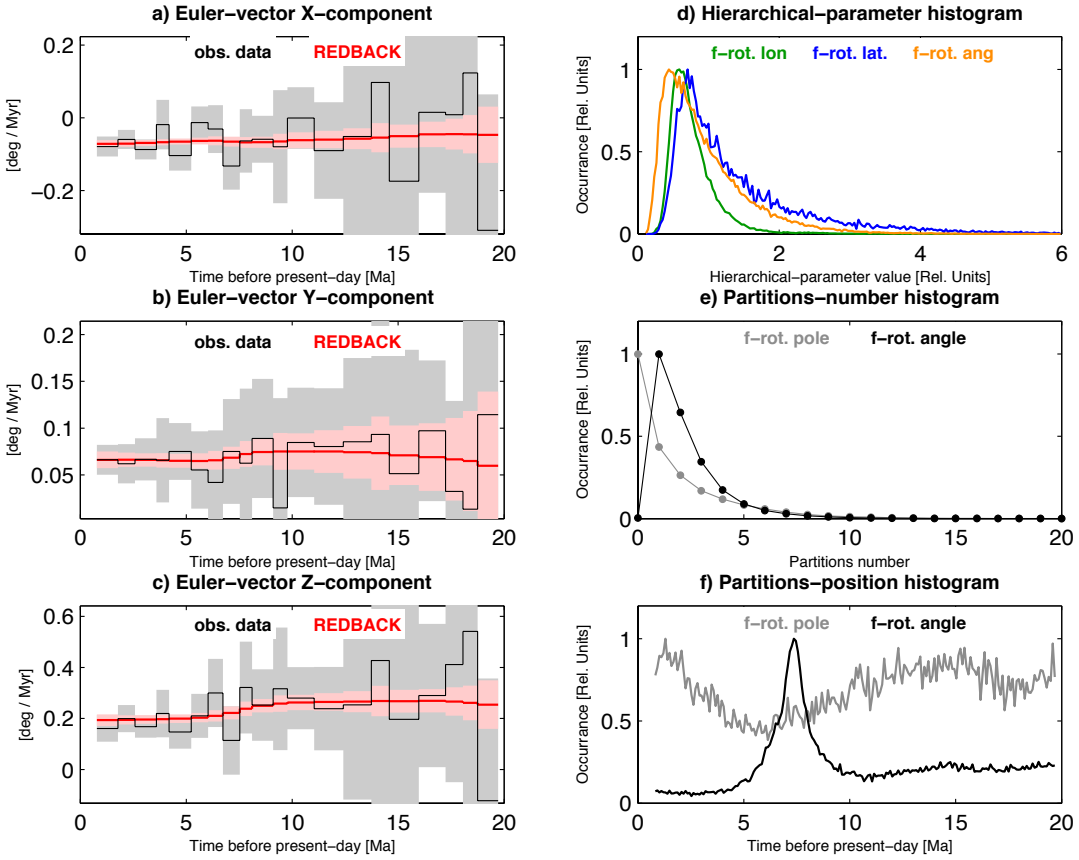

Figure 33: Diagnostics associated with step 14

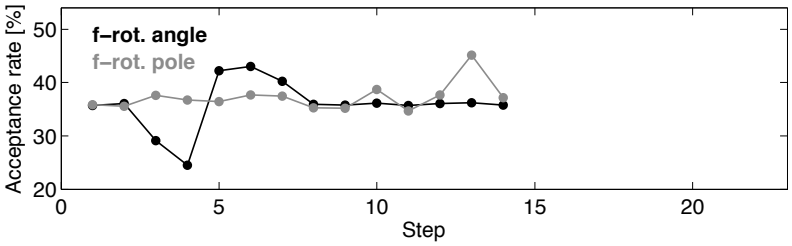

Figure 34: Progression of acceptance rates at step 14

8.15 Step 15

Figure 35 indicates that setting `time_sigma` = 0.1 yields a better result compared to that obtained at step 12, in terms of histograms smoothness, credible intervals as well as acceptance rates. At step 16 we test the impact of setting `time_sigma` = 3.

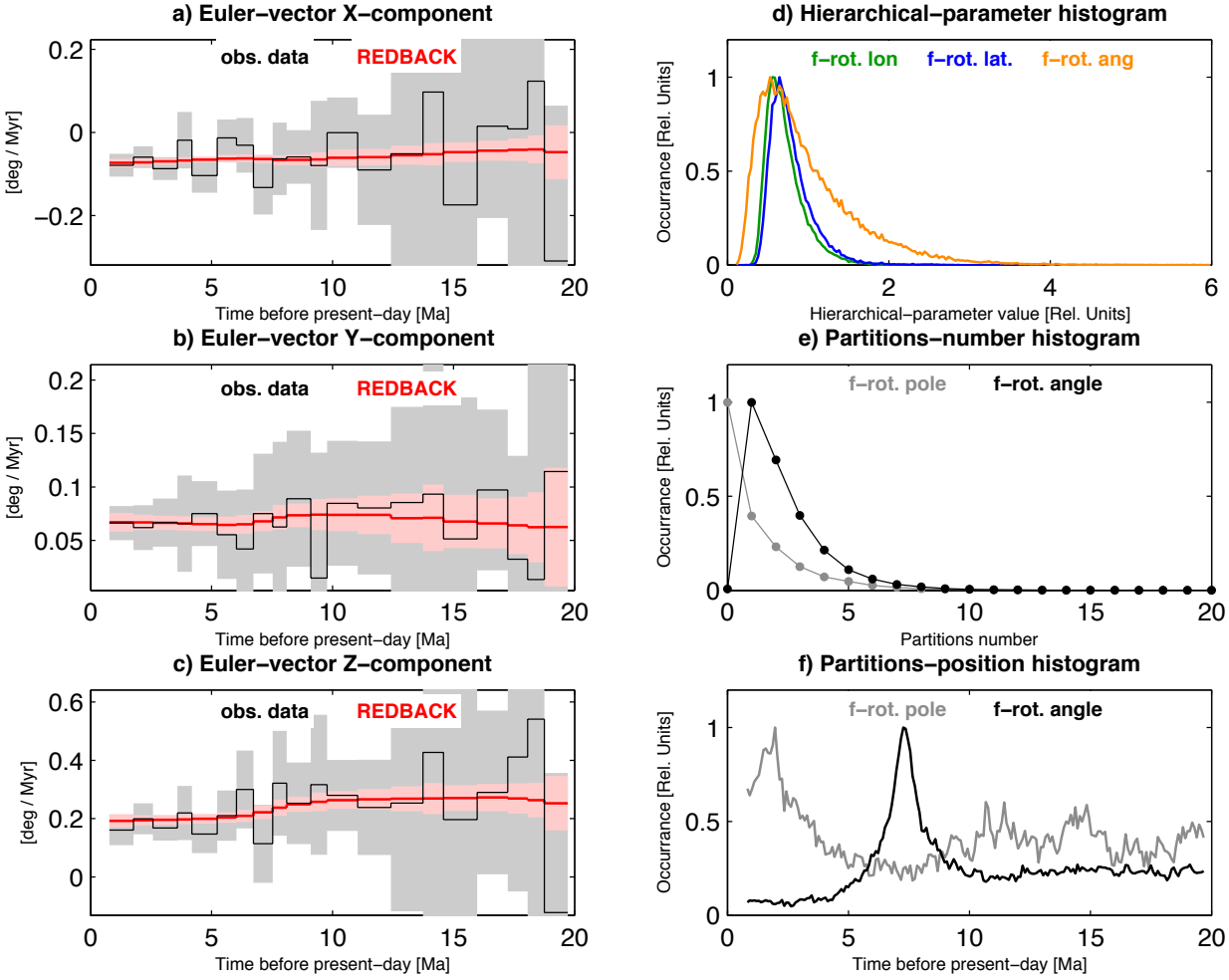

Figure 35: Diagnostics associated with step 15

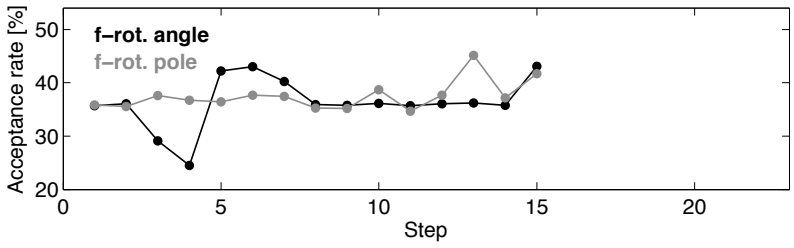

Figure 36: Progression of acceptance rates at step 15

8.16 Step 16

From the comparison of Figures 35 and 37 we decide to settle on settle on `time_sigma` = 0.1. Next, we begin refining the parameters that implement perturbation–options 1 and 3 in *Iaffaldano et al.* [2014]. That is, (i) those parameters determining by how much the magnitude of a single plate–motion change is varied from one accepted model to the next (`lon_sigma`, `lat_sigma` and `ang_sigma`), as well as (ii) the magnitude of a plate–motion change that is newly–cast into the next model (`lon_sigma_bd`, `lat_sigma_bd` and `ang_sigma_bd`). We start by refining the parameters associated with the rotated angle (`ang_sigma` and `ang_sigma_bd`). Further, we elect to consider `ang_sigma` = `ang_sigma_bd`, as well as `lon_sigma` = `lon_sigma_bd` and `lat_sigma` = `lat_sigma_bd` later on. We do so because there are no a–priori reasons to imagine that the distribution, across the model ensemble, of magnitudes of already–cast plate–motion changes should be different – in a statistical sense – from that of newly–cast changes. Of course, you are not prevented from testing independent values of `ang_sigma` and `ang_sigma_bd`. At step 17 we increase both `ang_sigma` and `ang_sigma_bd` from their default value (0.1) to 1.

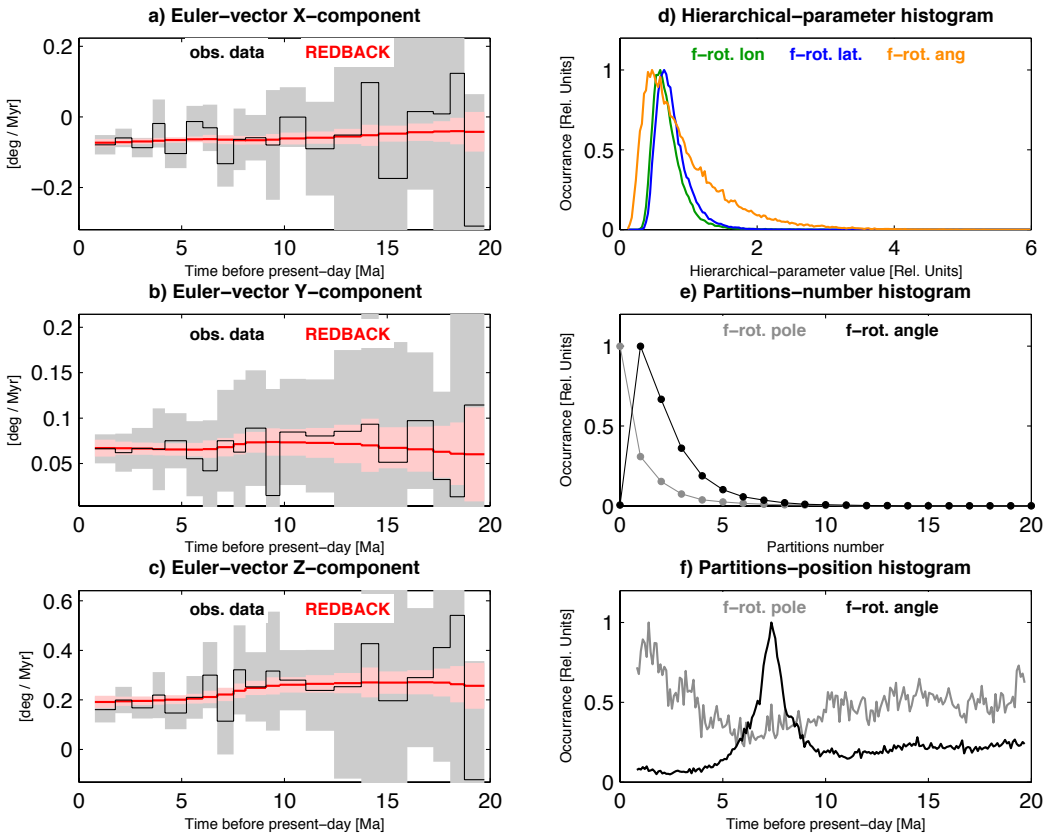

Figure 37: Diagnostics associated with step 16

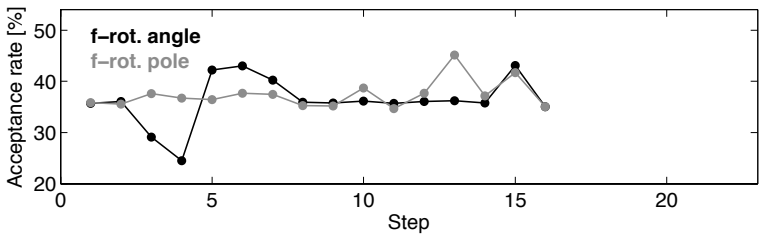

Figure 38: Progression of acceptance rates at step 16

8.17 Step 17

From the comparison of Figures 35 and 39 we determine that `ang_sigma` = `ang_sigma_bd` = 1 yields a worsening in terms of histograms smoothness (particularly in panel f) and credible intervals. At step 18 we explore the effect of `ang_sigma` = `ang_sigma_bd` = 0.01.

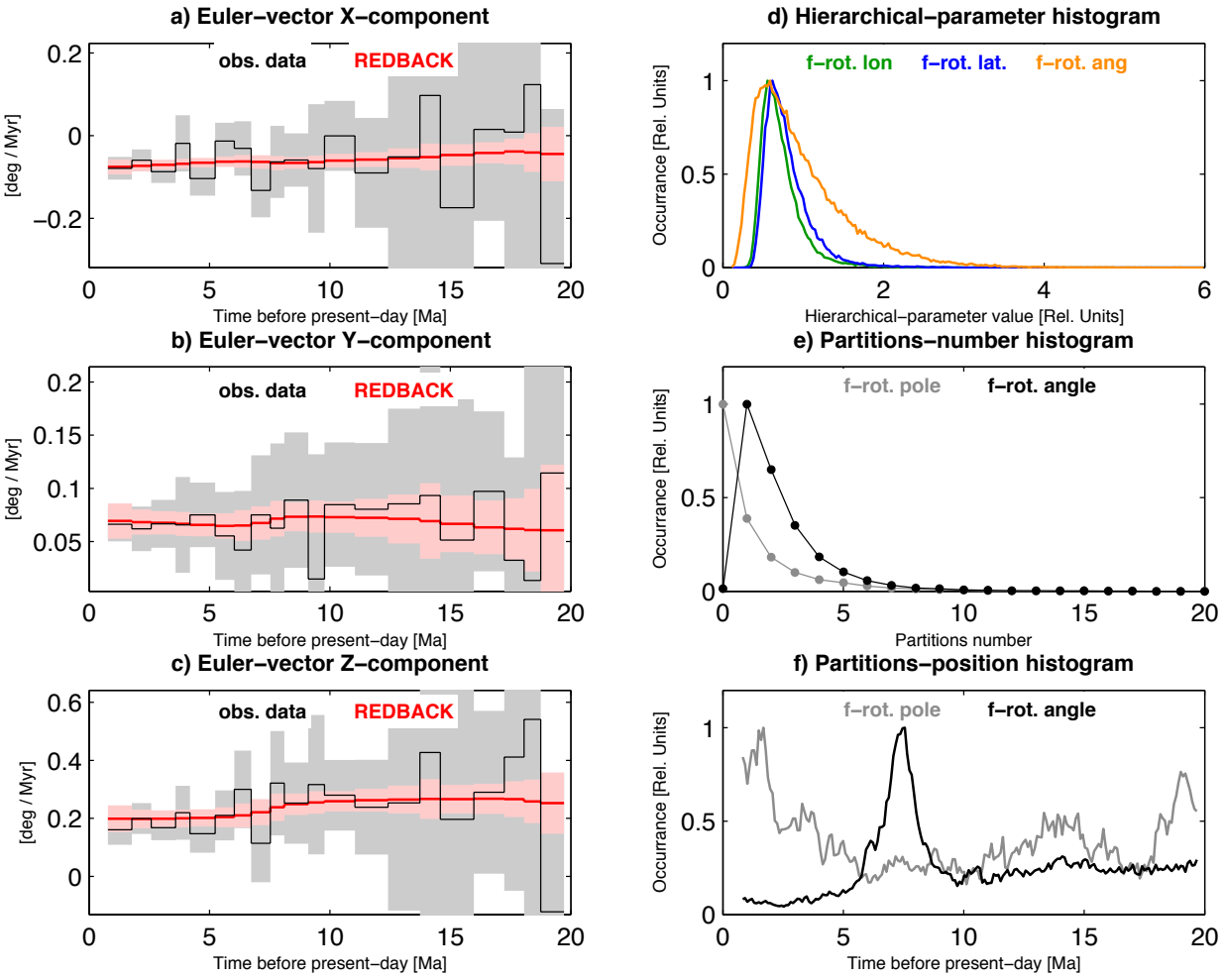

Figure 39: Diagnostics associated with step 17

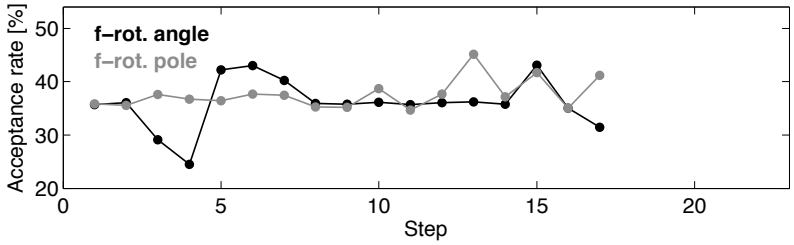

Figure 40: Progression of acceptance rates at step 17

8.18 Step 18

Setting `ang_sigma` = `ang_sigma_bd` = 0.01 seems to determine an improvement with respect to results at step 15, particularly for credible intervals. Therefore at step 19 we decrease them further 0.001.

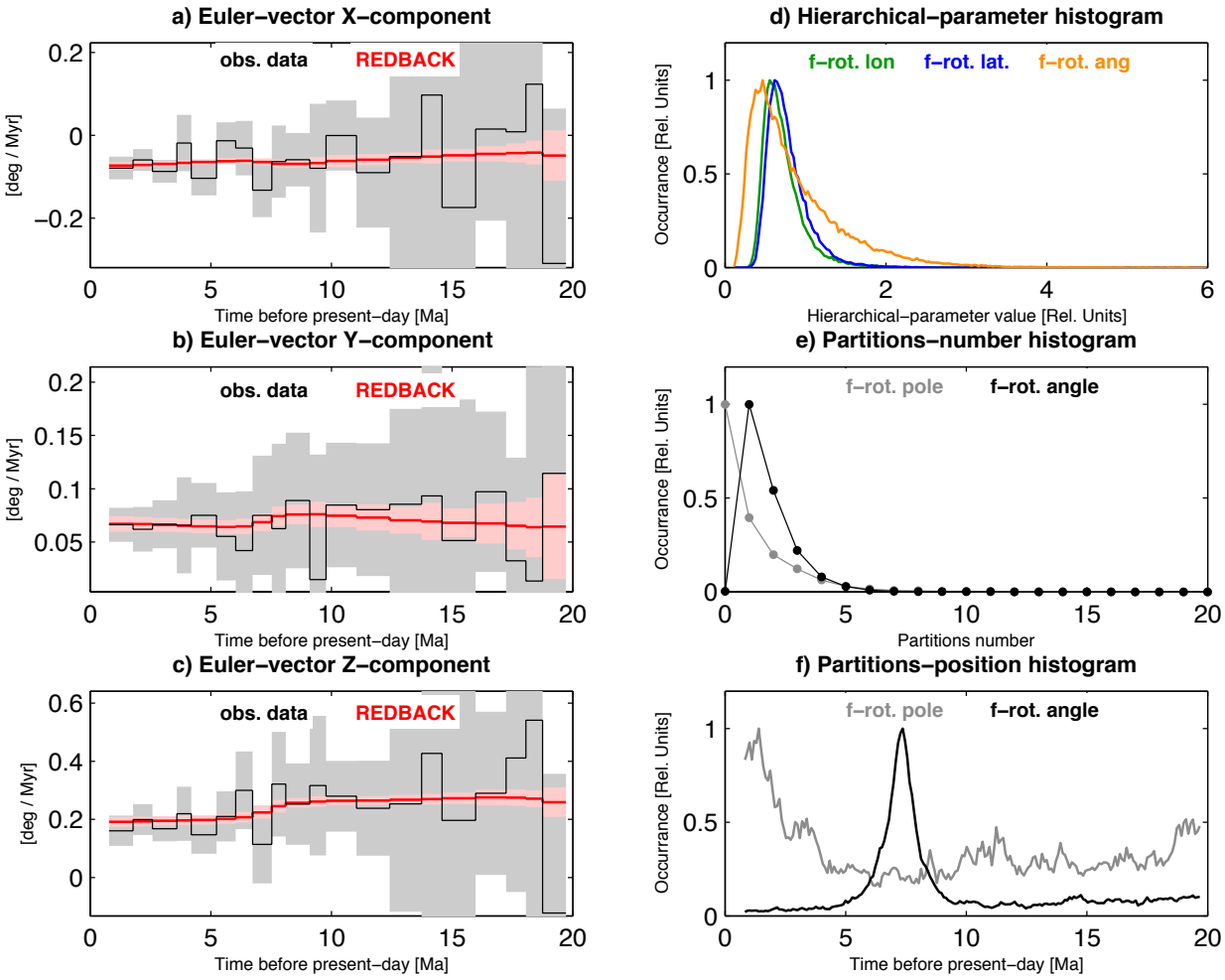

Figure 41: Diagnostics associated with step 18

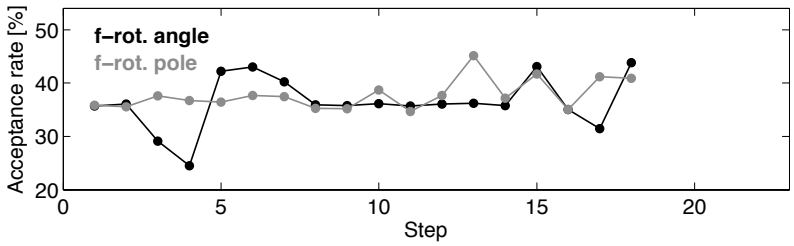

Figure 42: Progression of acceptance rates at step 18

8.19 Step 19

Setting `ang_sigma` = `ang_sigma_bd` = 0.001 clearly determines unreasonable sampling, as evidenced by panels d and f in Figure 43. Thus, we decide to settle on `ang_sigma` = `ang_sigma_bd` = 0.01. At step 20 we begin refining `lon_sigma` and `lon_sigma_bd` by decreasing their value from the default (1) to 0.1.

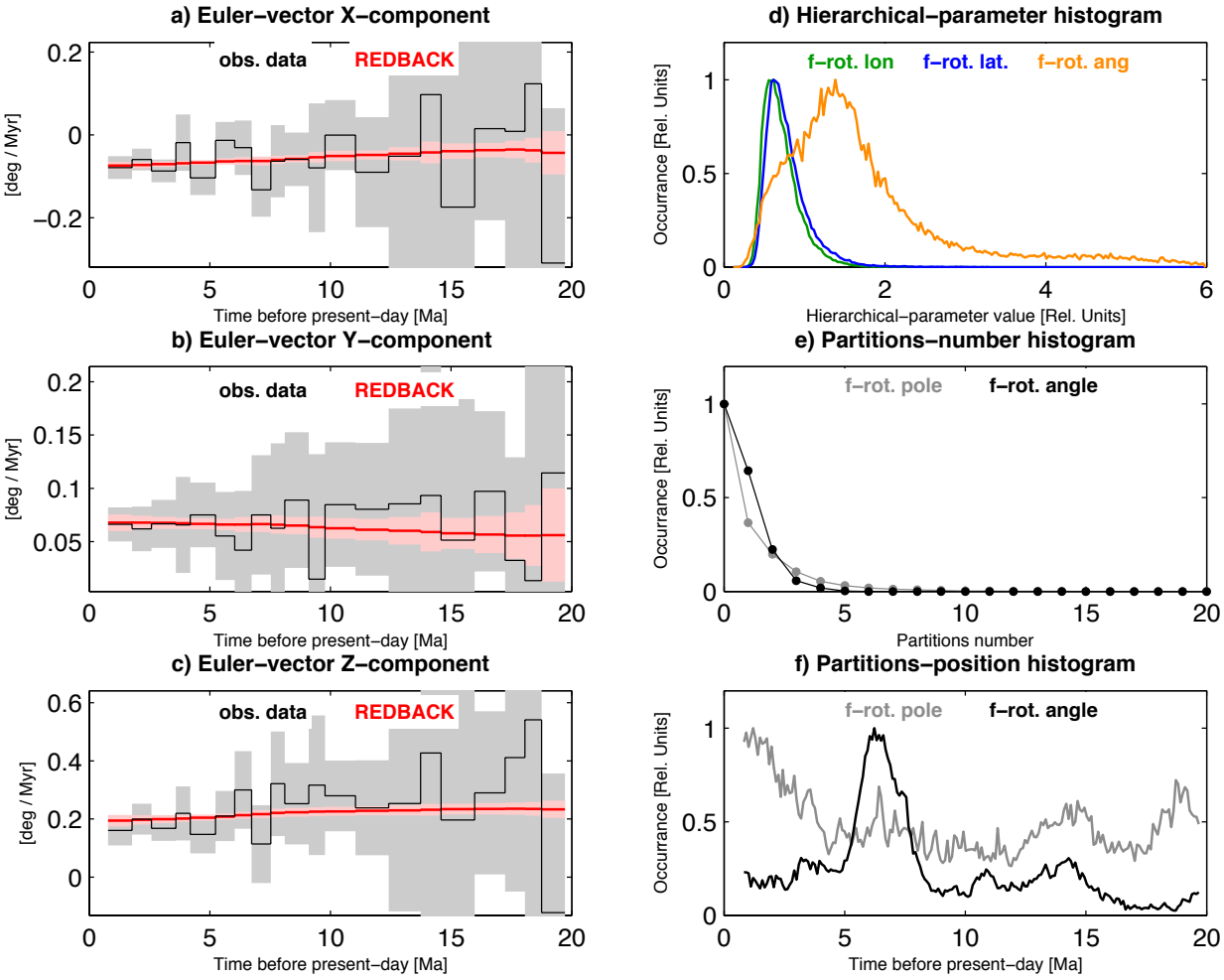

Figure 43: Diagnostics associated with step 19

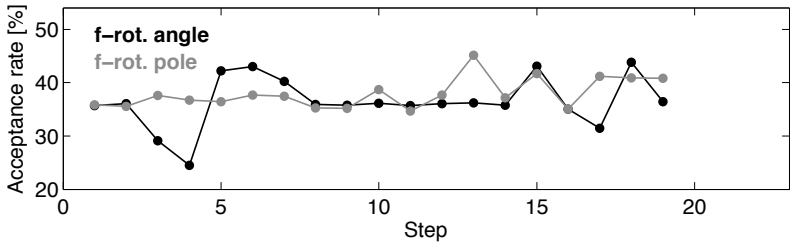

Figure 44: Progression of acceptance rates at step 19

8.20 Step 20

Although setting `lon_sigma` = `lon_sigma_bd` = 0.1 implies an increase in the acceptance rates (Figure 46), it also determines a worsening of the finite–rotation histograms in Figure 45f, compared to those in Figure 41f. At step 21 we test the impact of setting `lon_sigma` = `lon_sigma_bd` = 3.

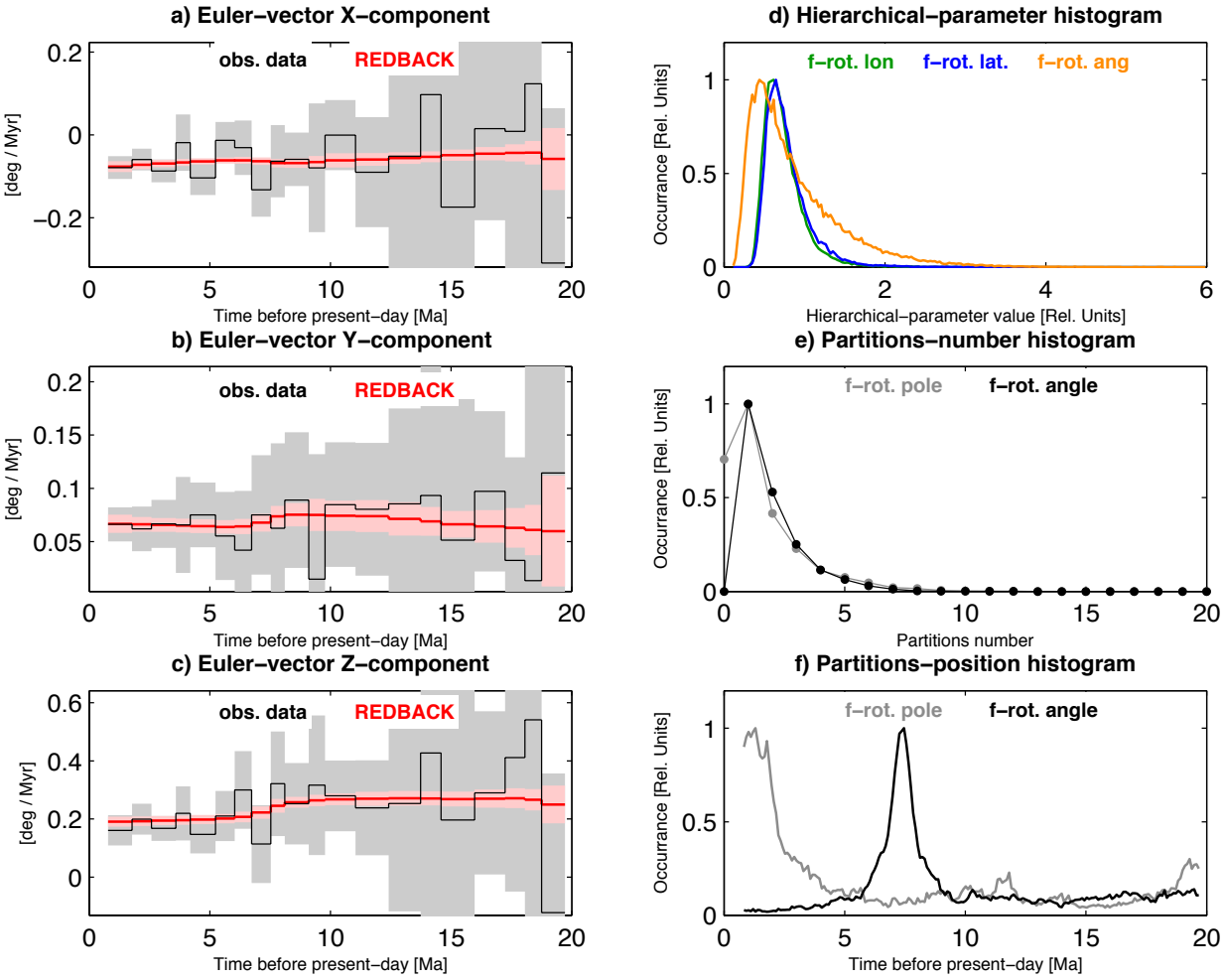

Figure 45: Diagnostics associated with step 20

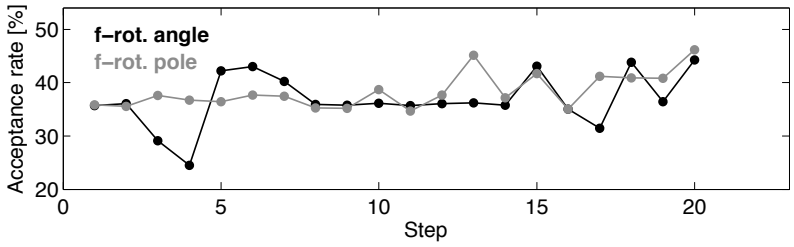

Figure 46: Progression of acceptance rates at step 20

8.21 Step 21

The result of setting `lon_sigma` = `lon_sigma_bd` = 3 seems fine in terms of histograms smoothness and acceptance rates. However, it is somewhat worse in terms of credible intervals, compared to the result at step 18 – where `lon_sigma` = `lon_sigma_bd` = 1. Therefore, at step 22 we settle on `lon_sigma` = `lon_sigma_bd` = 1. After running a few calculations yourself, you will find that reasonable sampling typically occurs when `lon_sigma` and `lon_sigma_bd` are set to a value equal to about 1/10 of the range covered by the longitude of finite–rotation poles in input (see Figure 4). For this reason, we leave `lat_sigma` and `lat_sigma_bd` equal to their default value (1), which corresponds to about 1/10 of the latitude range in input. You are, of course, encouraged to explore different values to convince yourself of the statement above.

Since we are happy with the parameter values chosen so far, the final step to take is to increase significantly `ensemble_size`. We do so in the hope that any further, second–order refinement of the input parameters we could have made is effectively compensated by sampling a larger number of model. At step 22, therefore, we also increase `ensemble_size` from 10^6 to $2{\cdot}10^7$.

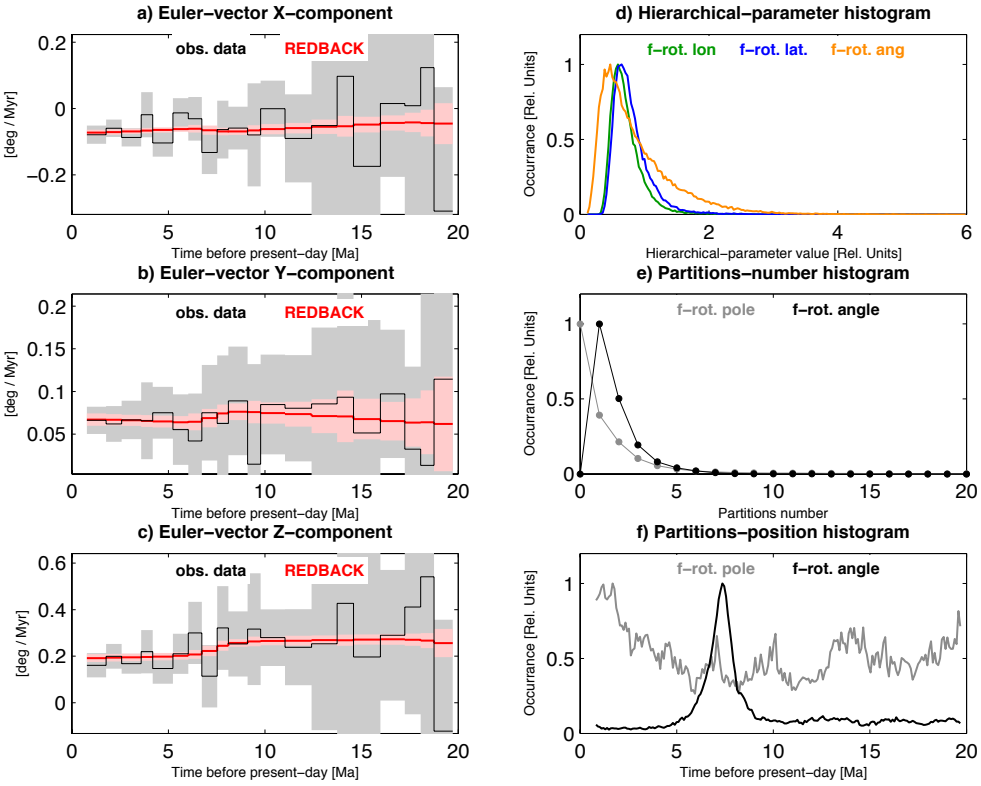

Figure 47: Diagnostics associated with step 21

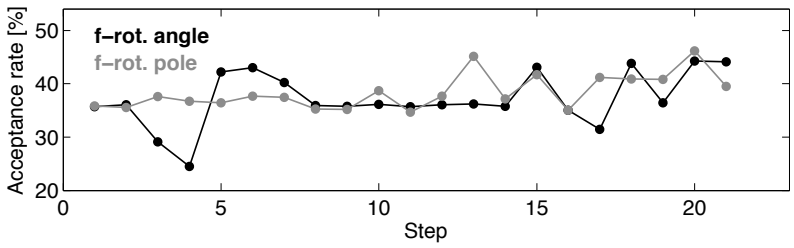

Figure 48: Progression of acceptance rates at step 21

8.22 Step 22

From the diagnostics associated with step 22 (Figure 49), we conclude that reasonable sampling of the model space has been achieved. This is evident in panel d, where histograms of the hierarchical parameters do present a smooth increase, a peak and a decrease to zero. It is also evident from panel f, from which we infer that there is one significant change in angular velocity, around 6–7 Ma. At the same time, the model ensemble warrants a continuous change of the finite–rotation pole. We also note that the single peak of the black profile in panel f is indeed in line with the fact that a partitions–number equal to 1 recurs most often across the ensemble (panel e, black profile). Lastly, Figure 50 shows that acceptance rates have overall increased to more satisfactory levels upon refinement of parameter values.

It is worth comparing these diagnostics to those obtained by using default values of all parameters but `ensemble_size`, which instead we set to $2 \cdot 10^7$. These are shown in Figure 51. The acceptance rates associated with such a calculation are 36% and 36.4% for finite–rotation angle and pole, respectively. These are essentially the same obtained at step 1 (see Figure 50). Note also that credible intervals in Figures 51a–c are much wider than those in Figures 49a–c. Such a comparison clearly demonstrates the usefulness of parameter refinement.

How good is the final solution provided by REDBACK *compared to the input finite rotations and associated stage Euler vectors? Iaffaldano et al.* [2012] demonstrated that stage Euler vectors for relative plate motions obtained through trans–dimensional hierarchical Bayesian Inference are indeed more plausible, in a geodynamical sense, than those associated with noisy finite rotations. In fact, rates at which torques need to vary in order to explain kinematic changes inferred through Bayesian Inference are smaller than estimates of those associated with tectonic and deep–mantle processes. The same is not true for kinematic changes inferred from noisy reconstructions. As to finite rotations, we test the quality of REDBACK solution against the very same magnetic anomaly identifications used by *Merkouriev and DeMets* [2008] to derive their finite rotations. This data set is available as part of a recently–established community infrastructure for marine magnetic identifications [*Seton et al.*, 2014]. Figure 52 shows a portion of this data set for the Atlantic ocean–floor north and south of Iceland. Dots represent magnetic identifications and are coloured according to the ages of the identified anomalies. Darker colours are identifications on the Eurasian plate, while lighter colours are identifications on the North American plate. We performed a simple and admittedly crude test where, for each reconstructed age, we rotated all identifications on the Eurasian side onto the North American side using both input and REDBACK finite–rotation sets. We then calculated distances between each rotated identification and the closest one that has been originally identified on the North American ocean–floor. In Figure 53 we plot the average of these distances for each reconstructed age. In black are the average distances obtained using the input finite rotations, while in red are those obtained using REDBACK finite rotations. Dashed areas indicate the intervals where 68% of the distances computed from all identifications available at a given age fall. From this simple comparison, we argue that finite rotations output by REDBACK are compatible with the observed pattern of ocean–floor magnetisation as much as those in input are. Charles DeMets (Univ. Wisconsin–Madison) very kindly performed a more rigorous test based on reduced χ^2, which indicates that the weighted root mean square (WRMS) associated with the REDBACK finite rotations increases by 50%, compared to the WRMS associated with the input finite rotations. *DeMets et al.* [2015a,b] performed independent, more stringent tests on the fit of outputs to original magnetisation and fracture–zone data in the North Atlantic and Southwest Indian Oceans. REDBACK satisfactorily passed these tests.

Lastly, within `EXAMPLES/`, inside the `REDBACK/` folder, you will also find `IN_SO_MD_G3_2006_FINITE_ROTATIONS.txt`, which contains finite rotations from *Merkouriev and DeMets* [2006] for the paleo–position of India with respect to Somalia since ∼20 Myr. You may try reducing noise in it, to familiarise yourself with REDBACK.

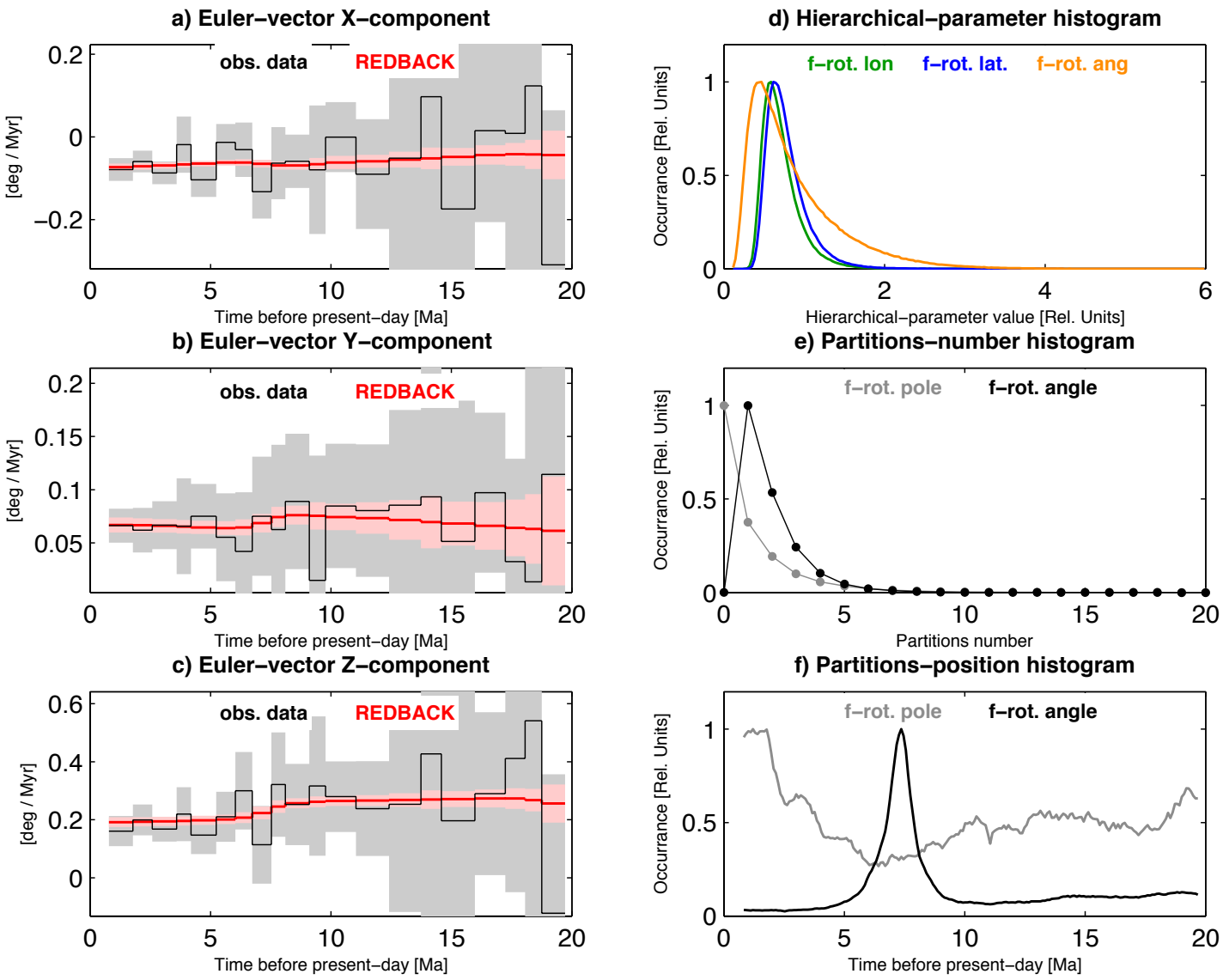

Figure 49: Diagnostics associated with step 22

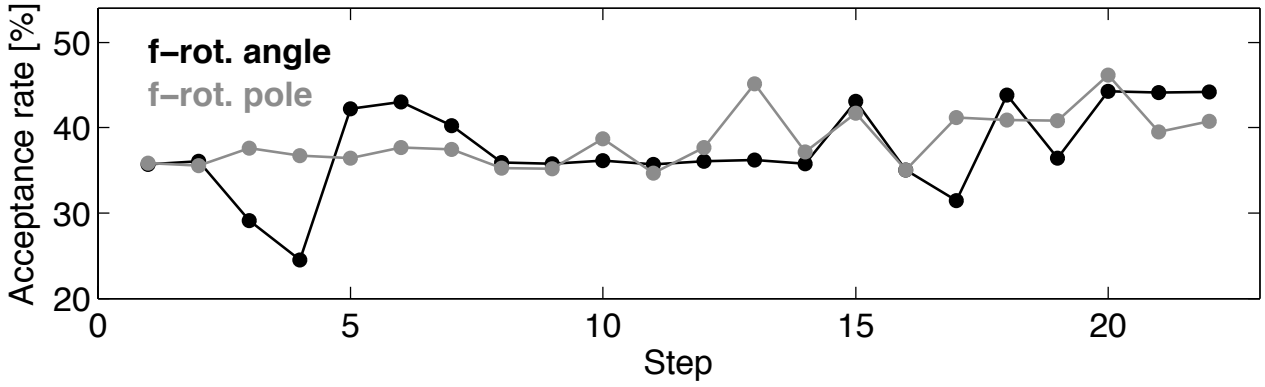

Figure 50: Progression of acceptance rates at step 22

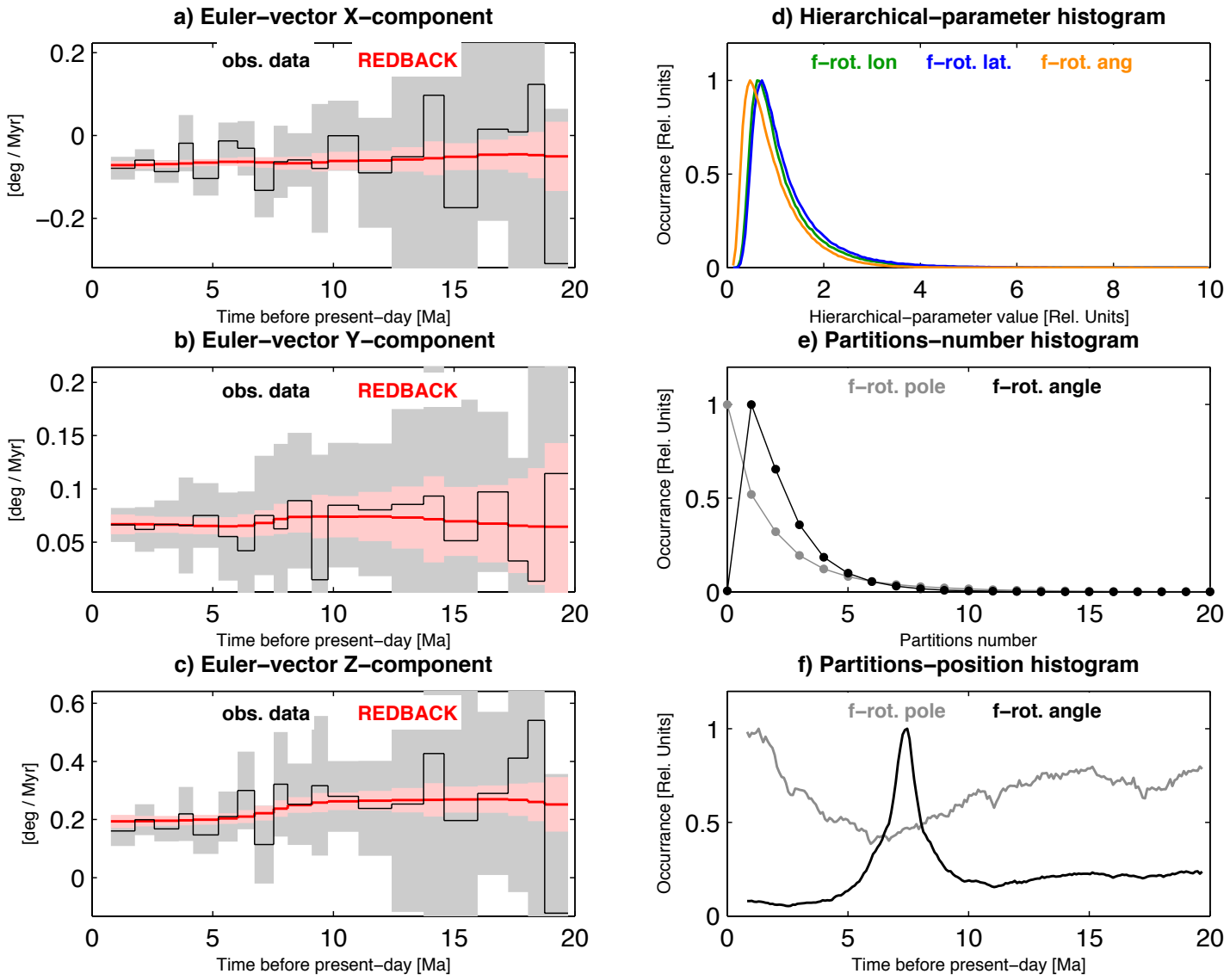

Figure 51: Diagnostics associated with a calculation performed using 20 million models and default values for all the other parameters.

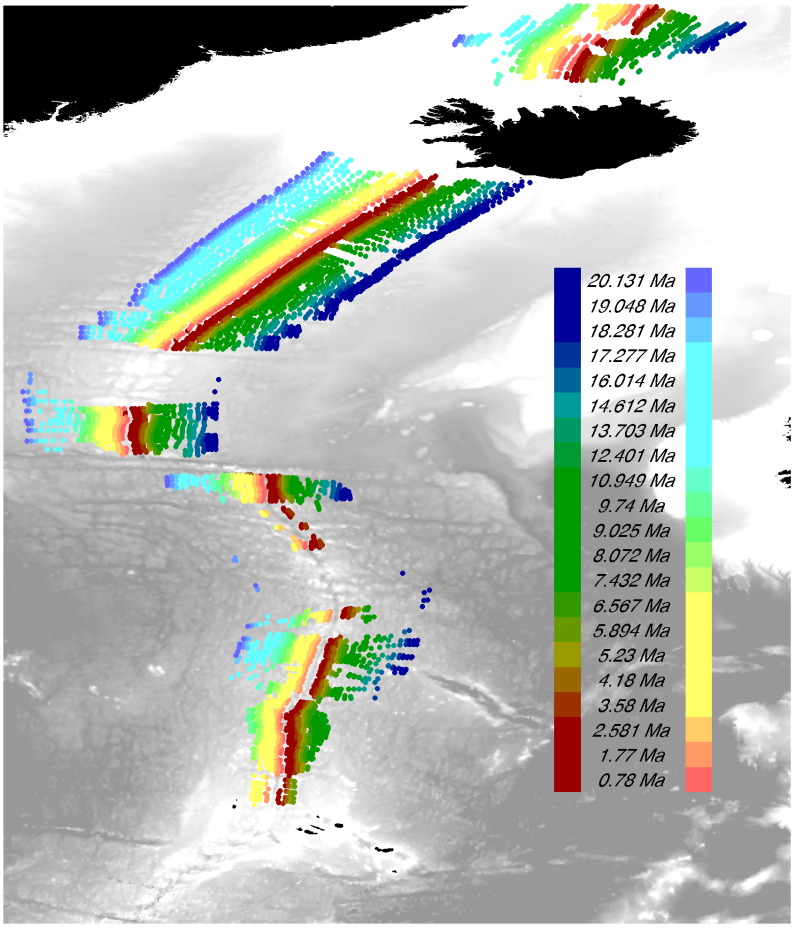

Figure 52: A portion of the data set of magnetic anomaly identifications (mainly south of Iceland) used by *Merkouriev and DeMets* [2008] to infer Eurasia/North America finite rotations since $\sim$ 20 Ma. Magnetic anomaly identifications are coloured according to the ages of the identified anomalies. In darker colours are identifications on the Eurasian ocean–floor, while lighter colours are those on the North America side. Ocean–floor bathymetry is in grey colour–scale, continents are in black.

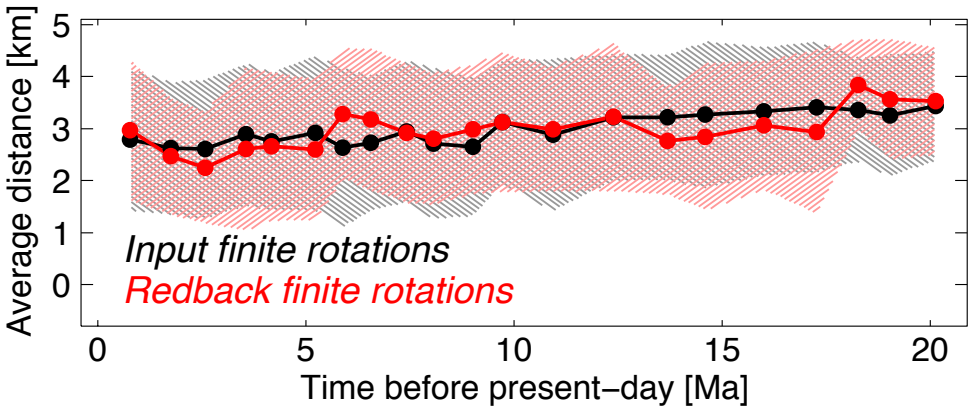

Figure 53: Average distance between magnetic anomaly identifications rotated from the Eurasian plate onto the North American plate – using input (in black) and REDBACK (in red) finite rotations – and those directly identified on the North American ocean–floor. Dashed areas show, for each identified age, intervals where 68% of the computed distances across the entire data set of *Merkouriev and DeMets* [2008] fall.

9 Final remarks

We hope that we were able to provide a clear description of how REDBACK works, what its capabilities are, and the way in which we suggest you refine the input parameters – although you are, of course, welcome to explore and find different ways of doing so.

We emphasise that we built into REDBACK the option of sampling the final solution (finite rotations and Euler vectors) at different time stages than the input data set. This is explicitly meant to facilitate the combination of different data sets. Such an option may be used, for instance, in determining the convergence between two plates from a plate circuit, or in assessing plate–circuit closure among three (or possibly more) plates. Given the effort one is required to put into refining the input parameter to ensure reasonable sampling, we realise that it may be tempting to first combine two or more finite–rotation data sets, and then use the result as input to REDBACK. We strongly discourage doing so. It is, in fact, not guaranteed that one set of input parameters that may have ensured reasonable sampling for either of the finite–rotation data sets, will do so for the other one(s), and thus for the combination of them.

We hope you will find REDBACK useful to your research, and welcome your feedback.

Giampiero Iaffaldano
Rhys Hawkins
Thomas Bodin
Malcolm Sambridge
Canberra, February 2014

10 Appendix A: Updates history

May 1, 2014

The input parameter `max_partitions` has been redefined. It now coincides with the number of plate–motion changes cast into models, rather than with such a number plus 1 (see Section 5.1 of the user manual).

This update involves both RJMCMC (up–to–date version is RJMCMC-1.0.7) and REDBACK (up–to–date version is REDBACK-1.0.2) tar-files, as well as the User Manual PDF-file.

June 18, 2014

An issue related to the output finite rotations (`OUTPUT_FINITE_ROTATIONS.txt`) has been fixed. The issue determined the potential presence of `NaN` (Not-a-Number) in the columns of longitude, latitude and angle of the finite rotations (particularly when sampling several million models) and was associated with redundancy of some operations.

This update involves only the REDBACK tar-file (up–to–date version is REDBACK-1.0.3).

October 22, 2014

The prior distribution of probability function for the rotated–angle models has been re–defined. It is set to be uniform within the minimum and maximum values of the *de–trended angle* time series (see Section 3, for more details), rather than the minimum and maximum values of the rotated–angle time series.

This is a major update that further improves the ability of REDBACK to distinguish kinematic changes that are likely to be true features of the data set, from those that are more likely to be associated with noise. It requires greater consideration of acceptance rates throughout the process of refining parameter values. For this reason, we dropped the example based on synthetic finite rotations, and revised the one base on real finite rotations (see Section 8) focusing also on the use of acceptance rates. This example has also been completed with a comparison of results against the record of ocean–floor magnetisation.

This update involves the REDBACK tar-file (up–to–date version is REDBACK-1.0.4) and the User Manual PDF-file.

March 3, 2015

This update fixes an issue associated with using the optional `input_time_file parameter`, which allows re–sampling the final solutions (Euler vectors and finite rotations) at user–specified times.

This update involves the REDBACK tar-file (up–to–date version is REDBACK-1.0.5).

November 12, 2015

This update involves only the REDBACK User Manual PDF-file. Subsection 4.1 features now a note on the need to input positive values of finite–rotation angles to REDBACK. Furthermore, Subsection 8.22 includes references to independent tests of the quality of REDBACK outputs.

References

Bull, J. M., C. DeMets, K. S. Krishna, D. J. Sanderson, and S. Merkouriev (2010), Reconciling plate kinematic and seismic estimates of lithospheric convergence in the central Indian Ocean, *Geology*, *38*, 307–310.

Cande, S. C., and D. V. Kent (1995), Revised calibration of the geomagnetic polarity timescale for Late Cretaceous and Cenozoic, *Journal of Geophysical Research*, *100*, 6093–6095.

Chang, T. (1988), Estimating the relative rotation of two tectonic plates from boundary crossings, *Journal of the American Statistical Association*, *83*, 1178–1183.

Cox, A., and R.-B. Hart (1986), *Plate tectonics: How it works*, Blackwell scientific publications.

DeMets, C., R. G. Gordon, and J.-Y. Royer (2005), Motion between the Indian, Capricorn and Somalian plates since 20 ma: implications for the timing and magnitude of distributed lithospheric deformation in the equatorial Indian ocean, *Geophysical Journal International*, *161*, 445–468.

DeMets, C., G. Iaffaldano, and S. Merkouriev (2015a), High–resolution Neogene and Quaternary estimates of Nubia–Eurasia–North America plate motion, *Geophysical Journal International*, *203*, 416–427.

DeMets, C., S. Merkouriev, and D. Sauter (2015b), High–resolution estimates of Southwest Indian Ridge plate motions, 20 Ma to present, *Geophysical Journal International*, *203*, 1495–1527.

Iaffaldano, G. (2014), A geodynamical view on the steadiness of geodetically–derived rigid plate–motions over geological time, *Geochemistry Geophysics Geosystems*, *15*, 238–254.

Iaffaldano, G., T. Bodin, and M. Sambridge (2012), Reconstructing plate–motion changes in the presence of finite–rotations noise, *Nature Communications*, *3:1048*.

Iaffaldano, G., R. Hawkins, T. Bodin, and M. Sambridge (2014), Redback: open–source software for efficient noise–reduction in plate kinematic reconstructions, *Geochemistry Geophysics Geosystems*, *doi: 10.1002/2014GC005309*.

Lourens, L., F. J. Hilgen, J. Laskar, N. J. Shackleton, and D. Wilson (2004), *A Geologic Time Scale*, pp. 409–440, Cambridge University Press, London.

Malinverno, A. (2002), Parsimonious Bayesian Markov chain Monte Carlo inversion in a nonlinear geophysical problem, *Geophysical Journal International*, *151*, 675–688.

Merkouriev, S., and C. DeMets (2006), Constraints on Indian plate motion since 20 ma from dense Russian magnetic data: Implications for Indian plate dynamics, *Geochemistry Geophysics Geosystems*, *7*(2), Q02,002.

Merkouriev, S., and C. DeMets (2008), A high-resolution model for Eurasia–North America plate kinematics since 20 ma, *Geophysical Journal International*, *173*, 1064–1083.

Royer, J.-Y., and T. Chang (1991), Evidence for relative motions between the Indian and Australian plates during the last 20 m.y. from plate tectonic reconstructions: Implications for the deformation of the Indo–Australian plate, *Journal of Geophysical Research*, *96*, 11,779–11,802.

Seton, M., J. M. Whittaker, P. Wessel, R. D. Muller, C. DeMets, S. Merkouriev, S. Cande, C. Gaina, G. Eagles, R. Granot, J. Stock, N. Wright, and S. Williams (2014), Community infrastructure and repository for marine magnetic identifications, *Geochemistry Geophysics Geosystems*, *15*, 1629–1641.